

Biodiversity and Evolutionary History of †*Lophionotus* (Neopterygii: †Semionotiformes) from the Western United States

Sarah Z. Gibson¹

Two species of the neopterygian genus †*Lophionotus* Gibson, 2013, are described. Specimens of †*Lophionotus chinleana*, new species, were previously and recently collected from freshwater deposits in the Upper Triassic Chinle Formation of Lisbon Valley, southeastern Utah. †*Semionotus kanabensis* Schaeffer and Dunkle, 1950, from lacustrine deposits in the Lower Jurassic Moenave Formation of southwestern Utah, is herein redescribed and attributed to the genus †*Lophionotus*, based on shared characters, including the infraorbital in the posteroventral corner of the orbit being expanded and contacting the anterior ramus of the preoperculum. Both new species of †*Lophionotus* are distinct from †*L. sanjuanensis* Gibson, 2013, in that they lack a postcranial hump, deep body, dense tuberculation, and ventrally expanded preoperculum. The addition of two new species lends to a revised generic description of the genus †*Lophionotus*. A phylogenetic analysis infers a monophyletic †*Lophionotus* sister to the genus †*Semionotus*, and †*Lophionotus* is placed within the family †*Semionotidae* within †*Semionotiformes*.

SEMIONOTIFORMES are a diverse group of extinct neopterygian fishes with a worldwide distribution in marine and continental deposits that range in age from the Middle Triassic (e.g., Deecke, 1889; Gardiner, 1993) to Cretaceous (e.g., Gardiner, 1993; Gallo and Brito, 2005; López-Arbarello and Codorniú, 2007; Forey et al., 2011). Fossil specimens which have been attributed to the family †*Semionotidae* have been described from Europe (e.g., Agassiz, 1833–1843; Fraas, 1861; Woodward, 1890; Larsonneur, 1964; Wenz, 1968; Wenz et al., 1994; Lambers, 1999), Asia (e.g., Su, 1996; Cavin and Suteethorn, 2006), Gondwana (e.g., López-Arbarello, 2004; López-Arbarello et al., 2008), and North America (e.g., Newberry, 1888; Schaeffer and Dunkle, 1950; McCune, 2004; López-Arbarello and Alvarado-Ortega, 2011; Gibson, 2013). One of the defining morphological characters of semionotids is the presence of prominent dorsal ridge scales (Olsen and McCune, 1991) and, like extinct and extant Lepisosteiformes (e.g., gars), their scales possess ganoin (Goodrich, 1907). The order †*Semionotiformes* has a complicated taxonomic history (Olsen and McCune, 1991; López-Arbarello, 2008), and, most recently, semionotid taxa have been included in several taxonomic revisions of holosteans that have focused on extinct and extant taxa in the closely related order Lepisosteiformes (e.g., Grande and Bemis, 1998; Cavin, 2010; Grande, 2010).

The taxonomic composition of the family †*Semionotidae* has been controversial. In Olsen and McCune's (1991) work on semionotids from the Newark Supergroup rock formations of Eastern North America, the family †*Semionotidae* was restricted to two genera, †*Lepidotes* and †*Semionotus*. Olsen and McCune (1991) proposed two synapomorphies that unite these genera within the family: 1) the presence of dorsal ridge scales and 2) the presence of a large posteriorly directed process on the epiotic. Within †*Semionotidae*, the number of suborbitals was used as the primary diagnostic character to distinguish between †*Semionotus* and †*Lepidotes* (McCune, 1986). Wenz (1999) proposed that the family †*Semionotidae* include the genera †*Semionotus*, †*Lepidotes*, †*Paralepidotus*, †*Araripelepidotes*, and †*Pliodes*. Wenz (1999) reevaluated morphological characters from previous studies (e.g., Patterson, 1975; Thies, 1989; Olsen and McCune, 1991; Gardiner et al., 1996) and included additional

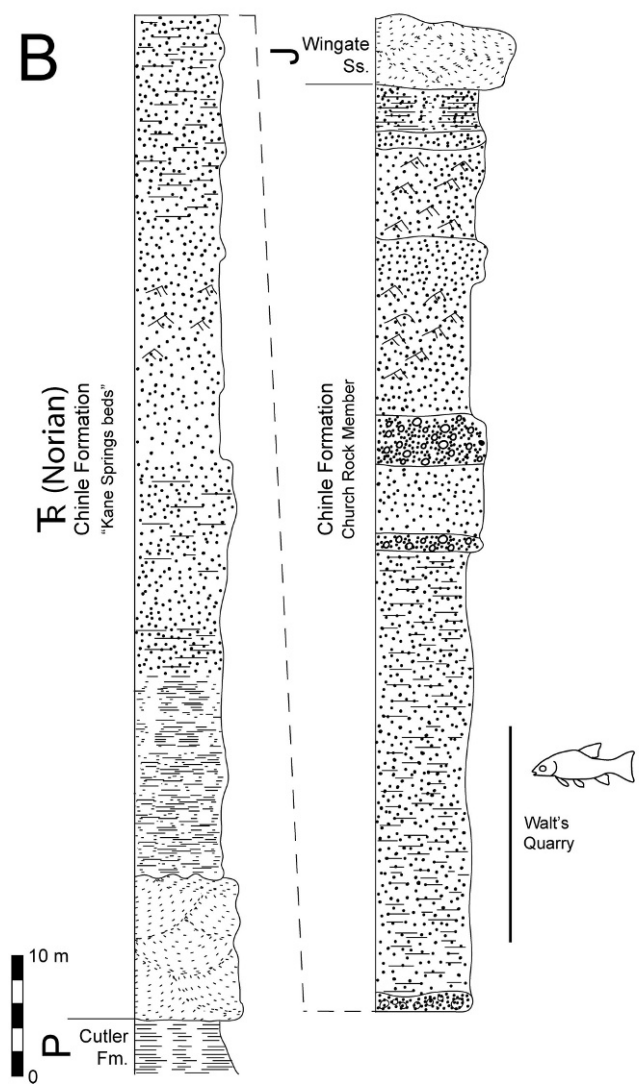
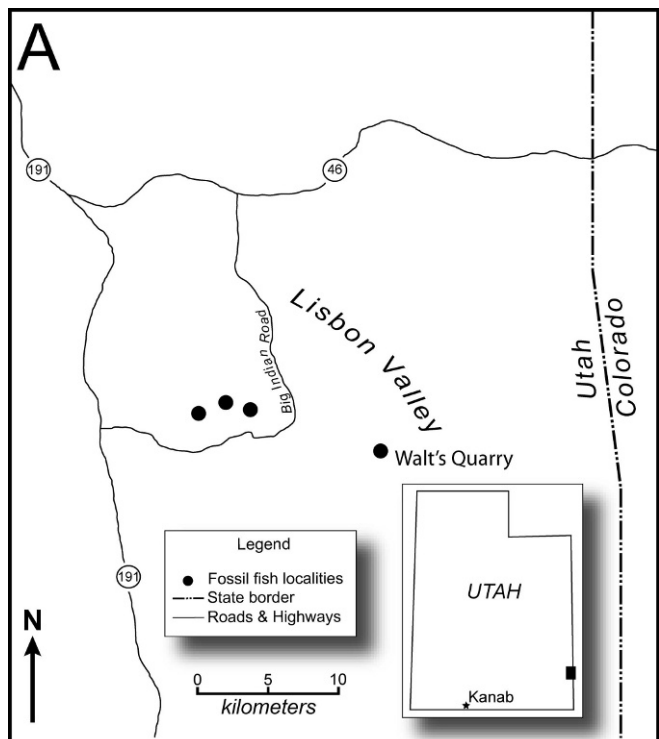
semionotiform taxonomic sampling; however, Wenz (1999) did not perform any character-based phylogenetic analysis, nor did she provide a new diagnosis for the family itself. Later parsimony-based studies of †*Semionotiformes* (Cavin and Suteethorn, 2006; Cavin, 2010) recovered a largely unresolved clade that includes semionotiform and lepisosteiform taxa, though the family †*Semionotidae sensu* Olsen and McCune (1991) was recovered as monophyletic when taxon sampling was limited to extinct species with the least amount of missing character data (Cavin and Suteethorn, 2006). Grande (2010) recovered the order †*Semionotiformes* as sister to Lepisosteiformes, but within †*Semionotiformes*, his taxonomic sampling was restricted to †*Semionotus*, excluding many other †*Semionotiformes* taxa, including †*Lepidotes*. However, Grande (2010) resurrected the term Holostei to include the Ginglymodi and Halecomorpha within Neopterygii. This was also supported by Xu and Wu (2012) in their parsimony-based analysis of neopterygian relationships. Xu and Wu (2012), however, limited their analysis to 15 taxa and did not provide a robust hypothesis of relationships within the order †*Semionotiformes*.

López-Arbarello (2012) provided the most comprehensive hypothesis of ginglymodian relationships to date. Using a matrix of 37 taxa and 90 morphological characters, López-Arbarello (2012) recovered a monophyletic †*Semionotiformes* based on five unambiguous synapomorphies, and restricted the family †*Semionotidae* to a single genus, †*Semionotus*. Other genera that were placed in †*Semionotidae* by Wenz (1999) and others, including †*Lepidotes*, were reexamined and placed in other groups within †*Semionotiformes* or Lepisosteiformes.

The first semionotiform fossils recorded in the western United States included fragments of scales, teeth, and fully articulated fish from deposits near Kanab, Utah (Eastman, 1917; Schaeffer and Dunkle, 1950). Schaeffer and Dunkle (1950) described and erected †*Semionotus kanabensis* (holotype AMNH 8870) from three-dimensional specimens collected near Kanab, Utah. These specimens were originally attributed to the Upper Triassic Chinle Formation (Schaeffer and Dunkle, 1950), but further investigation proved that the fully articulated specimens are from the younger, Lower Jurassic Moenave Formation (Schaeffer, 1967; Milner and

¹ Department of Geology, University of Kansas, 1345 Jayhawk Boulevard, Lawrence, Kansas 66045; E-mail: szgibson@ku.edu.
Submitted: 22 February 2012. Accepted: 4 February 2013. Associate Editor: W. L. Smith.

© 2013 by the American Society of Ichthyologists and Herpetologists DOI: 10.1643/CI-12-028



Kirkland, 2006). In overall body morphology, *†S. kanabensis* resembles other species of *†Semionotus*, such as a fusiform body, gently sloping dorsal border, and smooth dorsal ridge scales. However, elements of the skull differ between *†S. kanabensis* and other species of *†Semionotus*, such as the ventrally expanded infraorbital series, and new information regarding the biodiversity of western United States semionotiforms (Gibson, 2013) indicates that attributing this species to *†Semionotus* is in need of reexamination.

†Lophionotus sanjuanensis, a hump-backed ganoin fish from the Triassic, was identified and described as a new genus and species of semionotiform fish after recent fieldwork in the Upper Triassic Chinle Formation in Lisbon Valley (Fig. 1A), San Juan County, southeastern Utah (Gibson, 2013). Recent and past fieldwork in the Chinle Formation in Lisbon Valley has yielded a trove of semionotiform material. Geologically, the Chinle Formation in Lisbon Valley can be separated into two major sections. The lower gray, bentonitic beds (Fig. 1B) are localized and have not been given a formal designation, but they are recognized as belonging to the Kane Springs beds of Blakey and Gubitosa (1983), and are the lateral equivalent to the Upper Triassic Moss Back Member of the Chinle Formation to the south (Schaeffer, 1967). The Kane Springs beds contain numerous terrestrial and semi-aquatic vertebrate remains, including archosaurs, phytosaurs, metoposaurs, and possibly dinosauromorphs (e.g., Milner et al., 2006a). The upper beds are comprised of alternating layers of mudstone, siltstone, fine-grained sandstone, and conglomerate (Fig. 1B), and are recognized as the Church Rock Member of the Chinle Formation (Blakey and Gubitosa, 1983; Blakey, 1989). The fish-bearing beds are found within the Church Rock Member in red and pale-green, fine-grained sandstone layers that show cross-lamination (Fig. 1B). The Church Rock Member in Lisbon Valley is interpreted as a freshwater fluvial-deltaic-lacustrine system, with series of stream channel deposits and conglomerate channel lag deposits (Stewart et al., 1972; Blakey and Gubitosa, 1983; Dubiel, 1987; Blakey, 1989).

†Lophionotus sanjuanensis is a medium-sized semionotiform with a deep body morphology; large postcranial hump; dense tuberculation on skull roof and postcranial hump; short snout with broad frontals; and preoperculum with a short, broad, paddle-like ventral process (Gibson, 2013). A number of characters are shared between *†Lophionotus sanjuanensis* and specimens previously attributed to the Lower Jurassic *†Semionotus kanabensis* and new specimens recently collected in Utah from the Upper Triassic Chinle Formation that are described in this study, including a single anamestic suborbital and ventrally expanded infraorbitals. Upon further investigation the recently collected specimens from the Chinle Formation are hypothesized to be a new

Fig. 1. (A) Locality map of Lisbon Valley, Utah (indicated by black square on inset), showing localities (approximate) for specimens of *†Lophionotus chinleana*, new species. Walt's Quarry, the type locality for *†L. chinleana*, new species, is indicated. Kanab, Utah, the type locality for *†L. kanabensis*, is indicated on inset. (B) Generalized stratigraphic column for the Chinle Formation in Lisbon Valley, Utah. Specimens of *†L. chinleana*, new species, were collected from the Walt's Quarry horizon.

species of †*Lophionotus*. Additionally, specimens of †*Semionotus kanabensis* (Schaeffer and Dunkle, 1950) from the Lower Jurassic Moenave Formation are identified as belonging to the recently described genus †*Lophionotus* (Gibson, 2013) based on shared characters described herein.

The purpose of this study is to describe a new species of †*Lophionotus* from the Upper Triassic Chinle Formation. This study also provides an updated and thorough redescription and diagnosis of the Lower Jurassic †*Semionotus kanabensis* and designates it within the genus †*Lophionotus*. A revised diagnosis of †*Lophionotus* is provided to accommodate the new information from the inclusion of multiple species, and the phylogenetic placement of the genus †*Lophionotus* is tested to determine the evolutionary relationships of the genus within †*Semionotiformes*.

MATERIALS AND METHODS

Specimens described in this study are from the following institutions: American Museum of Natural History (AMNH), Smithsonian Institution (USNM), and the Natural History Museum of Utah (UMNH). Other material examined includes specimens from the following institutions: Field Museum of Natural History (FMNH), New Mexico Museum of Natural History and Science (NMMNHS), and St. George Dinosaur Discovery Site at Johnson Farm, Utah (SGDS). Comparisons were also made to semionotiform specimens in the literature (e.g., McCune, 1986, 1987; Olsen and McCune, 1991; Tintori and Lombardo, 2007; López-Arbarello, 2008). Daggers (†) indicate extinct taxa.

Preservation of specimens differs between the Upper Triassic Chinle Formation and Lower Jurassic Moenave Formation. Specimens from the Chinle Formation are compressed (flattened), usually in lateral aspect. Specimens in this study from the Moenave Formation are preserved three-dimensionally (mostly uncrushed in the skull region). However, the specimens from the Moenave Formation appear to have been weathered and eroded, and many surface details are worn from erosion. Preservation of specimens from the Chinle Formation varies: specimens were either exposed at the surface and weathered, or removed while quarrying, and were not subject to weather and erosion.

Fossil fish specimens from Lisbon Valley were prepared by the author, Andrew R. C. Milner, Robert Baldazzi, and Sally Stephenson. Specimens were mechanically prepared with pneumatic tools and microjacks to remove excess matrix from within a few millimeters above the specimen. The remainder of preparation was done with sharpened carbide needles to expose the specimen. In instances where only a negative impression of the fossil is preserved, a latex peel was made to provide a positive “cast” of the specimen.

Several stereomicroscopes with different resolution power were used. Photographs of the specimens were taken with a digital SLR camera with a macro-style lens. Drawings of the specimens were done with a *camera lucida* arm attachment and a digital drawing tablet over high-resolution photographs.

Terminology.—The terminology used herein follows the osteological terminology outlined by Schultze (2008) and Wiley (2008). Postcranial morphology follows the terminology outlined in Arratia (2008). In instances where terminology has varied in the literature over the years, the traditional terminology is presented here in parentheses: parietals (frontals), postparietals (parietals), infraorbitals posterior to

orbit (postinfraorbitals), infraorbitals below orbit (subinfraorbitals), posttemporal (suprascapulars), anterior infraorbitals (lachrymals or lacrimals), temporal canal (postorbital or otic canal). The infraorbitals are described by position relative to the orbit, rather than numbered, to avoid potential homology problems (see Jollie, 1986).

Anatomical abbreviations.—a.io, anterior infraorbital (lacrimals); ang, angular; ar, articular; bchst, branchiostegal; bf, basal fulcra; b.pr, branched principal ray; ch, ceratohyal; cl, cleithrum; d.scu, dorsal scute; d, dentary; dpt, dermopterotic; dsph, dermosphenotic; ecp, ectopterygoid; enp, endopterygoid; ex, extrascapular; ff, fringing fulcra; HL, head length, measured from tip of snout to posterior end of operculum; io, infraorbital; iop, interoperculum; n, nasal; mx, maxilla; MBD, maximum body depth, measured from dorsal to ventral margins at the deepest portion of the body; op, operculum; p.bf, paired basal fulcra; p.ff, paired fringing fulcra; p, parietal (frontal); pcl, postcleithrum; pmx, premaxilla; pop, preoperculum; pp, postparietal (parietal); part, prearticular; pr, principal ray; psph, parasphenoid; psp, postspiracular; ptt, posttemporal; q, quadrate; qj, quadrato-jugal; rar, retroarticular; SL, standard length, measured from tip of snout to the posterior end of the vertebral column; scl, supracleithrum; so, supraorbital; sop, suboperculum; suo, suborbital.

Taxonomic and morphological character sampling for phylogenetic analysis.—For this study, all three species of †*Lophionotus* were coded for the 90 characters included in López-Arbarello (2012) analysis of extinct and extant ginglymodian evolutionary relationships. Taxonomic sampling for this study included the 37 representatives of extinct and extant actinopterygian fishes included in the study by López-Arbarello (2012), as well as †*L. sanjuanensis*, †*L. chinleana*, new species, and †*L. kanabensis*.

The following is an abbreviated list of morphological characters from López-Arbarello (2012). In instances where the character was taken or modified from another study by López-Arbarello (2012), the initial source of the character is indicated. For a more detailed description and discussion of these characters, please refer to López-Arbarello (2012).

1. Relative position of the dorsal fin: dorsal fin contained between pelvic and anal fins (0), dorsal fin opposite to anal fin (1), dorsal fin opposite to pelvic fins (2), dorsal fin originates anterior to pelvic fins and extends opposite to anal fin (3).
2. Posttemporal fossa (Coates, 1999: character 33): absent (0), present (1).
3. Forward extension of the exoccipital around the vagus nerve (Olsen and McCune, 1991: character 3): absent (0), present (1).
4. Opistotic (Wiley, 1976: character 6c): present (0), absent (1).
5. Intercalar (Olsen, 1984: character 22): present (0), absent (1).
6. Basisphenoid (Wiley, 1976: character 17b): present (0), absent (1).
7. Sphenotic with small dermal component (Grande, 2010: character 23): absent (0), present (1).
8. Posterior myodome (Wiley, 1976: character 2a): present (0), absent (1).
9. Elongation of the rostral region anterior to the lower jaw symphysis (Grande, 2010: character 4): extends

anterior to the dentary symphysis by less than 20% of mandibular length (0), extends well anterior to the dentary symphysis by more than 50% of mandibular length (1).

10. Vomers co-ossified (Olsen, 1984: character 38): absent (0), present (1).
11. Autopalatine missing (Wiley, 1976: character 11b): absent (0), present (1).
12. Ectopterygoid elongate (Wiley, 1976: character 10b): absent (0), present (1).
13. Ectopterygoid participation in palatal surface area (Grande, 2010: character 63): ectopterygoid form half or less of the palatal region (0), ectopterygoid forms the majority of the palatal region (1).
14. Part of dorsal surface of ectopterygoid ornamented and forming part of skull roof (Grande, 2010: character 61): absent (0), present (1).
15. Endopterygoid dentition: present (0), absent (1).
16. Quadrat position in front of the orbit (Wiley, 1976: character 13b): absent (0), present (1).
17. Splint-like quadratojugal (modified from Brito, 1997: character 32): absent (0), present and independent (1), present and partially fused to the quadrate (2), completely fused to the quadrate (3).
18. Symplectic involvement in jaw joint (Grande and Bemis, 1998: character 61): does not articulate with lower jaw (0), distal end articulates with articular bone of lower jaw (1).
19. Ornamentation of the dermal bones of the skull (Grande, 2010: character 2, Grande and Bemis, 1998: character 8): ornamented with tubercles or ridges (0), smooth or very slightly ornamented (1), ornamented with firmly anchored large conical teeth (2).
20. Number of extrascapular bones (modified from Grande and Bemis, 1998: character 49): one pair (0), two pairs (1), three or more pairs (2).
21. Posterior extension of postparietals median to the single pair of laterally placed extrascapular bones: character 21): absent (0), present (1).
22. Relative length of postparietals (parietals) and parietals (frontals): length of postparietals less than half but more than one-third the length of parietals (0), length of postparietals about half the length of parietals (1), length of postparietals less than one-third the length of parietals (2).
23. Length of parietals (frontals) (from Jain, 1983; modified from Grande and Bemis, 1998: character 34): less than 3 times longer than their maximum width (0), 3 or more times longer than their maximum width (1).
24. Parietal (frontal) bones distinctly broader posteriorly, but long and narrow anteriorly (modified from Arratia, 1999: character 188): absent (0), present (1).
25. Antorbital portion of parietal (frontal): broad (0), tapering gradually (1), tubular (2).
26. Parietal (frontal) ethmoidal sagittal lamina: absent (0), present (1).
27. Triangular lateral expansion of antorbital portion of parietal (frontal): absent (0), present (1).
28. Nasals long and narrow: absent (0), present (1).
29. Circumorbital ring (Wiley, 1976: character 9a): supraorbitals do not contact infraorbitals at the anterior rim of the orbit (0), supraorbitals contact infraorbitals, closing the orbit (1).
30. Ventral border of infraorbital series flexes abruptly dorsally at the anterior margin of the orbit: absent (0), present (1).
31. Large supraorbital bones: absent (0), present (1).
32. Most anterior supraorbital bone trapezoidal, longest at ventral margin, and contacting more than one infraorbital bone on ventral margin: absent (0), present (1).
33. A series of toothed infraorbitals bordering the snout (Wiley, 1976: character 3b): absent (0), present (1).
34. Anterior infraorbitals (Olsen and McCune, 1991: character 1): absent (0), present (1).
35. Most anterior infraorbital: lower than or equaling the posterior elements (0), deeper than posterior elements (1).
36. Relative size of the infraorbital bone (or bones) at the posteroventral corner of the orbit: not enlarged (0), enlarged, but do not reach the preoperculum (1), enlarged and reach the preoperculum (2).
37. Shape of the infraorbital bones at the posterior border of the orbit: deeper than long, sometimes almost tubular (0), approximately quadrangular (1), longer than deep, expanded posteriorly (2).
38. Dermosphenotic participation in orbital margin (Grande, 2010: character 16): dermosphenotic reaches orbital margin (0), dermosphenotic does not reach orbital margin (1).
39. Dermosphenotic/sphenotic association (Grande, 2010: character 22): closely associated with each other (i.e., contacting or fused to each other) (0), not in contact with each other (1).
40. Quadrat laterally covered by infraorbital bones: absent (0), present (1).
41. Suborbital bones (Grande and Bemis, 1998: character 7): present (0), absent (1).
42. Number of suborbital bones (modified from Cavin and Suteethorn, 2006: character 4): one (0), two (1), several arranged in one row, which extends anteriad below the orbit (2), mosaic of numerous suborbitals (3), three or four suborbitals arranged in a row, which does not extend anteriad below the orbit (4).
43. Independent of the total number, there is a large suborbital covering almost the whole area between the infraorbital bones and the preoperculum (López-Arbarello, 2012): absent (0), present (1).
44. First and last suborbitals are larger than the other suborbitals: absent (0), present (1).
45. Suborbital series separates preoperculum from dermopterotic: absent (0), present (1).
46. Triangular suborbital lateral to quadrate: absent (0), present (1).
47. Premaxilla with nasal process (modified from Olsen and McCune, 1991: character 4): absent (0), present (1).
48. Premaxillary nasal process forming an external dermal component of the skull roof (Wiley, 1976: character 5b): absent (0), present (1).
49. Supraorbital canal in premaxillary nasal process (Wiley, 1976: character 4b): absent (0), present (1).
50. Length of maxilla: long, extends backward lateral to the coronoid process of the lower jaw (0), short, does not reach the coronoid process (1), atrophied or absent (2).
51. Depth of maxilla: shallow (0), deep (1).
52. Supramaxilla (Wiley, 1976: character 3a): absent (0), present, single bone (1), present, two bones (2).
53. Maxillary teeth (Cavin, 2010: character 30): present (0), absent (1).
54. Plicidentine (Wiley, 1976: character 27b): absent (0), present (1).

55. Tritoral dentition (from Jain, 1983): absent (0), moderately tritoral (1), extremely tritoral (2).

56. Well-developed posteroventral process of the dentary (from Thies, 1989): absent (0), present (1).

57. Double row of teeth in dentary (modified from Grande, 2010: character 39): absent (0), present (1).

58. Mandibular symphysis very deep (from Jain, 1983): absent (0), present (1).

59. Extent of teeth on dentary (excluding coronoid tooth plates) (Grande, 2010: character 56): tooth row extends over a third the length of dentary (0), tooth row is present on only the anterior one third or less of dentary (1).

60. Shape of preoperculum: dorsoventrally elongated without anteroventral arm (0), crescent-shaped (1), L-shaped (2).

61. Exposure of dorsal limb of preoperculum (Grande, 2010: character 73): mostly exposed forming a significant part of the ornamented lateral surface of the skull anterior to the operculum (0), entirely covered or nearly entirely covered by other dermal bones in adults (1).

62. Posterior border of preoperculum notched ventrally: absent (0), present (1).

63. Shape of the operculum: subrectangular, deeper than long (0), rounded to quadrate, approximately as deep as long (1), tapering anteroventrally (2).

64. Suboperculum with well-developed ascending process: absent (0), present (1).

65. Shape of ascending process of the suboperculum: robust, with broad base and rounded distal end (0), slender, tapering dorsad (1).

66. High ascending process of the suboperculum: less than or equal to half of the length of the dorsal border of the bone (0), more than half of the length of the dorsal border of the bone (1).

67. Suboperculum less than half the depth of the operculum: absent (0), present (1).

68. Interoperculum (modified from Wiley, 1976: character 10a): absent (0), present (1).

69. Size of interoperculum: large, approximately as long as the ventral arm of the preoperculum (0), small, remote from mandible (1).

70. Gular plate (modified from Olsen and McCune, 1991: character 8): double (0), single (1), absent (2).

71. Opistocoelous vertebrae (Wiley, 1976: character 26b): absent (0), present (1).

72. Knob-like anteroventral process of posttemporal: absent (0), present (1).

73. Supracleithrum with a concave articular facet for articulation with the posttemporal (Grande, 2010: character 93): absent (0), present (1).

74. Series of denticles along the ridge between the branchial and lateral surfaces of the cleithrum (from Bartram, 1977): absent (0), one or two rows (1), several rows (2).

75. Fringing fulcra on pectoral fin: present (0), absent (1).

76. Fringing fulcra on pelvic fin: present (0), absent (1).

77. Large dorsal fin, with more than 20 rays: absent (0), present (1).

78. Large basal fulcra in the dorsal and anal fins: absent (0), present (1).

79. Scale-like ray at the dorsal margin of the caudal fin (from Bartram, 1977): absent (0), present (1).

80. A constant number of exactly eight lepidotrichia in the lower, non-axial lobe of the tail (from Bartram, 1977): absent (0), present (1).

81. A constant number of exactly six lepidotrichia in the lower, non-axial lobe of the tail: absent (0), present (1).

82. Body lobe scale row (modified from Lombardo and Tintori, 2008): absent (0), present, with additional incomplete row (1), present, without additional incomplete row (2).

83. Dorsal ridge of scales (modified from Olsen and McCune, 1991: character 17): inconspicuous (0), conspicuous, with a low spine (1), conspicuous, with a deep spine (2).

84. Scales of the body with a strong posteriorly directed spine: absent (0), present (1).

85. Vertical peg-and-socket articulation: present (0), reduced or absent (1).

86. Longitudinal articulation of the scales of the body: absent (0), single (1), double (2).

87. Posttemporal penetration by lateral line canal (Grande, 2010: character 91): present (0), absent (1).

88. Supraorbital sensory canal in parietal (modified from Wiley, 1976): supraorbital canal penetrates parietals at the central portion of these bones (0), supraorbital canal running almost on the lateral rim of the parietals (1), supraorbital canal does not penetrate the parietals (2).

89. Orbital canal (sensory canal present in supraorbital bones): absent (0), present (1).

90. Deep groove housing the middle pit line in dermopterotic and parietal: absent (0), present (1).

No character definitions from López-Arbarello (2012) were modified in this study; however, additional specimens of †*Semionotus capensis* examined yielded new information, and the following characters have been modified from López-Arbarello (2012) for †*S. capensis*: character 19, '?' changed to '1'; character 28, '?' changed to '1'; character 36, '?' changed to '1'; character 50, '?' changed to '0'; character 51, '?' changed to '0'; character 52, '?' changed to '1'. Further examination of specimens of †*Semionotus elegans* indicates the assignment of character 30 from '?' to '1'; additionally, specimens of †*S. elegans* examined in this study were observed to possess a triangular lateral expansion on the anterior of the parietals (frontals), resulting in a change of coding from '0' to '1'. The morphological character state matrix is presented in Table 1.

Phylogenetic analyses of morphological data.—The dataset used for this study was assembled in Mesquite version 2.75 (Maddison and Maddison, 2010). A parsimony analysis was performed with TNT version 1.1 (Goloboff et al., 2008) with 20 independent heuristic searches and tree-bisection-reconnection (TBR) branch swapping. Characters were treated as unordered and of equal weight. Polymorphisms are treated as multistate. Symmetric resampling bootstraps (Goloboff et al., 2003) were performed with 100 replicates in TNT, with group frequencies presented. The subholosteian genus †*Perleidus* was designated the outgroup, with the following genera acting as functional outgroups for the analysis: halecomorphs †*Watsonulus eugnathoides* and *Amia calva*; stem teleosts †*Leptolepis coryphaenoides*, †*Pholidophorus bechei*, and †*Siemensichthys macrocephalus*; and †*Dapedium*.

Table 1. Morphological Data Matrix of 90 Characters Modified from the Investigation of López-Arbarello (2012). Polymorphisms are indicated by a cell with more than one state.

	1	2	3	4	5	6	7	8	9	10	11	12	13	14	15	16	17	18	19	20	21	22	23	24	25
† <i>Perleidus</i>	0	1	0	0	0	0	?	0	0	?	0	?	?	?	?	0	0	?	0	0	0	0	0	0	
† <i>Watsonulus</i>	0	1	0	?	0	0	?	0	0	0	0	0	0	0	0	0	0	0	0	0	0	0	0	0	
<i>Amia</i>	3	1	0	1	0	0	0	0	0	0	0	0	0	0	0	0	0	0	0	1	0	0	0	0	
† <i>Leptolepis</i>	?	?	0	0	0	0	0	0	0	0	1	?	0	0	0	0	0	0	0	0	0	0	0	0	
† <i>Pholidophorus</i>	2	1	0	0	0	0	0	0	0	0	0	1	?	0	0	0	0	0	0	0	2	1	0	0	
† <i>Siemensichthys</i>	2	?	?	?	?	?	?	0	0	0	?	0	0	?	?	?	?	?	0	3	0	0	0	0	
† <i>Dapedium</i>	0	0	0	0	0	0	0	0	0	0	0	0	0	0	0	0	0	0	0	0	0	0	0	0	
<i>Lepisosteus</i>	1	0	0	0	0	0	0	0	0	0	0	0	0	0	0	0	0	0	0	0	0	0	0	0	
† <i>Attractosteus</i>	1	0	0	0	0	0	0	0	0	0	0	0	0	0	0	0	0	0	0	0	0	0	0	0	
† <i>Masillosteus</i>	1	?	?	?	?	?	?	0	0	?	?	0	0	?	?	?	?	?	0	0	1	0	0	0	
† <i>Obaichthys</i>	1	0	1	1	1	1	1	?	0	1	0	?	0	0	?	0	0	2	1	0	0	0	0	0	
† <i>Dentilepisosteus</i>	1	0	1	1	1	1	1	?	1	1	1	0	?	0	1	0	?	0	1	0	0	0	0	0	
† <i>Pliodetes</i>	2	?	?	?	?	?	?	0	0	?	0	0	?	0	0	?	?	?	0	2	1	0	0	0	
† <i>Araripelepidotes</i>	2	1	?	?	?	?	?	?	?	?	?	?	?	?	?	?	?	?	0	1	1	0	0	0	
† <i>Isanichthys</i>	1	?	?	?	?	?	?	?	?	?	?	?	?	?	?	?	?	?	0	0	2	1	0	0	
† <i>Scheenstia maximus</i>	0	?	?	?	?	?	?	0	0	?	0	0	?	0	0	?	?	?	0	0	1	0	0	0	
† <i>Scheenstia laevis</i>	0	?	?	?	?	?	?	0	0	?	0	0	?	0	0	?	?	?	0	0	1	0	0	0	
† <i>Scheenstia mantelli</i>	0	1	1	1	1	1	1	?	0	0	?	0	0	?	0	0	?	?	0	0	1	0	0	0	
† <i>Scheenstia zappi</i>	0	?	?	?	?	?	?	?	0	0	?	0	0	?	0	0	?	?	0	0	1	0	0	0	
† <i>Lepidotes semiserratus</i>	0	?	?	?	?	?	?	?	0	0	?	0	0	?	0	0	?	?	0	0	1	0	0	0	
† <i>Neosemionotus</i>	0	?	?	?	?	?	?	?	0	0	?	0	0	?	0	0	?	?	0	0	1	0	0	0	
† <i>Callipurbeckia minor</i>	0	?	?	?	?	?	?	1	?	?	0	?	0	?	0	?	?	1	0	0	1	0	0	0	
† <i>Tlayuamichin</i>	0	?	?	?	?	?	?	1	?	?	0	?	0	?	0	?	?	0	0	0	1	0	0	0	
† <i>Macrosemimimus</i>	0	?	?	?	?	?	?	0	0	?	0	0	?	0	0	?	0	0	0	1	0	0	0	0	
† <i>Macrosemimimus</i>	0	?	?	?	?	?	?	1	?	?	0	1	?	?	?	0	0	?	0	0	1	0	0	0	
<i>lennieri</i>	0	1	0	1	?	1	?	1	1	?	1	?	1	?	1	?	0	0	?	0	0	1	0	2	
† <i>Semionotus bergeri</i>	0	?	1	?	1	1	?	?	1	?	1	?	?	0	0	?	0	0	1	0	1	0	0	1	
† <i>Semionotus elegans</i>	0	?	1	?	1	1	?	?	0	?	0	?	0	?	0	0	?	0	1	0	1	0	0	1	
† <i>Semionotus capensis</i>	0	?	?	?	?	?	?	?	0	?	0	?	0	?	0	?	?	0	1	0	1	0	0	2	
† <i>Paralepidotus</i>	3	?	?	?	?	?	?	?	?	?	?	?	?	?	?	?	?	?	?	?	0	1	0	0	
† <i>Semolepis</i>	0	?	?	?	?	?	?	?	?	?	?	?	?	?	?	?	?	?	0	1	0	0	1	0	
† <i>Macrosemius</i> spp.	3	?	?	?	?	?	?	?	1	1	?	?	?	?	?	?	?	?	0	1	2	0	1	0	
† <i>Notagogus</i> spp.	3	?	?	?	?	?	?	?	1	0	?	?	?	?	?	?	?	?	1	2	1	0	0	2	
† <i>Propterus</i> spp.	3	?	?	?	?	?	?	?	1	0	?	?	?	?	?	?	?	?	1	2	1	0	0	0	
† <i>Sangjiorioichthys sui</i>	0	?	?	?	?	?	?	?	0	?	0	?	0	?	0	0	?	?	0	1	0	0	1	0	
† <i>Luoxiongichthys aldae</i>	0	?	?	?	?	?	?	?	0	?	0	?	0	?	0	0	?	?	0	0	0	0	0	0	
† <i>Lophionotus sanjuanensis</i>	0	?	?	?	?	?	?	?	0	?	0	?	0	?	0	0	?	?	0	1	0	0	0	0	
† <i>Lophionotus chinleana</i>	0	?	?	?	?	?	?	?	0	?	0	?	0	?	0	0	?	?	0	1	0	0	0	0	
† <i>Lophionotus kanabensis</i>	0	?	?	?	?	?	?	?	0	?	0	?	0	?	0	0	?	?	0	0	0	0	0	1	

Table 1. Continued.

Table 1. Continued.

Table 1. Continued.

Neopterygii Regan, 1923

Ginglymodi Cope, 1872 [*sensu* Grande, 2010]
 †Semionotiformes Arambourg and Bertin, 1958 [*sensu* López-Arbarello, 2012]
 †*Lophionotus* Gibson, 2013

Type species.—†*Lophionotus sanjuanensis*, Gibson, 2013.

Revised generic diagnosis.—Small- to medium-sized semionotiform fish; single, narrow anametic suborbital (multiple suborbitals in genera such as †*Tlayuamichin*, †*Macrosemimimus*, †*Callipurbeckia*, and †*Sangiorgioichthys*); deep ventral infraorbitals that expand below suborbital and contact the anterior ramus of the preoperculum (narrow infraorbitals in †*Semionotus*); closed circumorbital ring (open circumorbital ring in †*Callipurbeckiidae*, †*Macrosemiidae*); parietals less than three times longer than their maximum width (long parietals in †*Semionotus*); two supraorbitals (three or more present in genera such as †*Semionotus*, †*Macrosemimimus*, †*Callipurbeckia*, and †*Tlayuamichin*); anterior supraorbital narrow and of equal to greater length than posterior supraorbital (supraorbitals of approximately equal length in genera such as †*Macrosemimimus*); gape of mouth small (as compared to Lepisosteidae); maxilla short and dentelous (as compared to genera such as †*Sangiorgioichthys*, †*Paralepidotus*, †*Tlayuamichin*, and †*Macrosemimimus*) styliform teeth on maxilla, premaxilla, and dentary (as opposed to tritoral dentition seen in †*Semiolepis*, †*Paralepidotus*, †*Macrosemimimus*, †*Tlayuamichin*, and †*Callipurbeckia*); lacks dermal component of sphenotic (dermal component of sphenotic present in †*Semionotus*).

†*Lophionotus chinleana*, new species

Chinle Ridgeback
 Figures 2–5, Table 1

†*Semionotus* sp. Schaeffer, 1967:317–319, pl. 21

Holotype.—UMNH VP 19417 (field number LV05-51): specimen in left lateral view (Figs. 2AB, 3, 4).

Paratypes.—UMNH VP 19418 (field number LV05-100): nearly complete specimen in left lateral view, missing fins and caudal peduncle (Fig. 2CD); AMNH 5682: specimen in left lateral view, missing anterior portion of skull (Schaeffer, 1967:pl. 21 number 5; Fig. 5). AMNH 5683A,B; UMNH VP 19415A, B (field number LV05-12); UMNH VP 19428 (field number LV05-17).

Specific diagnosis.—The diagnosis for this species is based upon the unique combination of the following characters: infraorbitals below the orbit deep, becoming narrower anteriad (infraorbitals below orbit in †*Lophionotus sanjuanensis* remain deep); presence of narrow infraorbital posterior to orbit (no posterior infraorbital in †*L. kanabensis*); narrow preoperculum with vertical dorsal arm (more anteriorly inclined in †*L. kanabensis*); ventral arm of preoperculum long and as equal to slightly wider than dorsal arm (short, broad ventral arm in †*L. sanjuanensis*); suborbital rectangular and wedge-shaped (suborbital large and rectangular in †*L. kanabensis*); one pair of lateral extrascapulars and one median extrascapular (one pair of

extrascapulars in †*L. sanjuanensis* and †*L. kanabensis*); presence of postspiracular (absent in †*L. sanjuanensis* and †*L. kanabensis*); gently curved dorsal body border (lacking postcranial hump seen in †*L. sanjuanensis*); small body size (average SL is 68 mm as compared to average SL of 87.7 mm in †*L. sanjuanensis* and 50–60 mm SL in †*L. kanabensis*); lacking dense tuberculation (dense tuberculation seen in †*L. sanjuanensis*).

Description.—†*Lophionotus chinleana*, new species, is a small fusiform fish with gently curved dorsal and ventral body borders. Average standard length (SL) of †*L. chinleana* is 69 mm, with an average maximum body depth (MBD) of about 26 mm. Skull is triangular in shape and slightly longer than deep. Average head length (HL) of †*L. chinleana* is about 18.3 mm, about 26% of the SL. Ratio of MBD to SL in †*L. chinleana* is about 37%.

Skull roof contains a pair of parietals and postparietals. Parietals are wide, shorter than species of †*Semionotus*, and comprise majority of skull roof (Figs. 2–5). Anterior margin is digitate and articulates with ascending process of premaxilla (Figs. 2BD, 4). Parietals are widest at posterior margin, constrict over the orbits, and taper slightly anterior to the antorbital process. Suture between parietals is weakly digitate. Parietals articulate with supraorbitals laterally, postparietals posteriorly, and dermopterotic dorsolaterally (Figs. 2–5).

Postparietals are rectangular, slightly longer than wide. Postparietals articulate with parietals anteriorly, dermopterotics laterally, and extrascapulars posteriorly (Figs. 2–5).

Dermopterotic is rectangular and longer than deep. Anterior margin slightly narrower than posterior margin. Small notch on posterodorsal margin at articulation of dermopterotic and postparietal; notch is convex on dermopterotic and concave on postparietal (Figs. 2–5). Dorsal border curves slightly anteroventrad and articulates with posteroventral corner of the parietal (Fig. 4). Dermopterotic articulates anteriorly with dermosphenotic, ventrally with preoperculum and suborbital, and posteriorly with extrascapular (Figs. 2–5).

Single pair of lateral extrascapulars posterior to postparietals. A median extrascapular is visible on UMNH VP 19417 (Figs. 2B, 3, 4) and AMNH 5682 (Fig. 5). Anterior margin of extrascapulars articulates with postparietals and dermopterotics in a smooth suture. Lateral extrascapulars are trapezoidal in shape, wider at lateral margin and tapering mediad (Figs. 3, 4). Surface of extrascapulars smooth (lacking ornamentation or tuberculation).

Posttemporals are best preserved in UMNH VP 19417 (Figs. 2AB, 3, 4) and AMNH 5682 (Fig. 5). They lie posterior to extrascapulars and triangular in shape, tapering mediad. A small anteroventral process articulates with dorsal margin of operculum. This process is slightly concave posteriorly and articulates with postspiracular between posttemporal and supracleithrum (Figs. 2–5).

Specimens UMNH VP 19417 and UMNH VP 19418 contain poorly preserved snout; however, both specimens preserve paired nasals (Figs. 2–4). Median rostral bone cannot be interpreted in any specimen. Nasal is small without a distinctive shape, and sits above the ascending process of the premaxilla (Fig. 4).

Antorbital bone is thin, long, and sits above the premaxilla. It articulates posteriorly with anterior infraorbitals (lacrimals) and curves at approximately a 90-degree

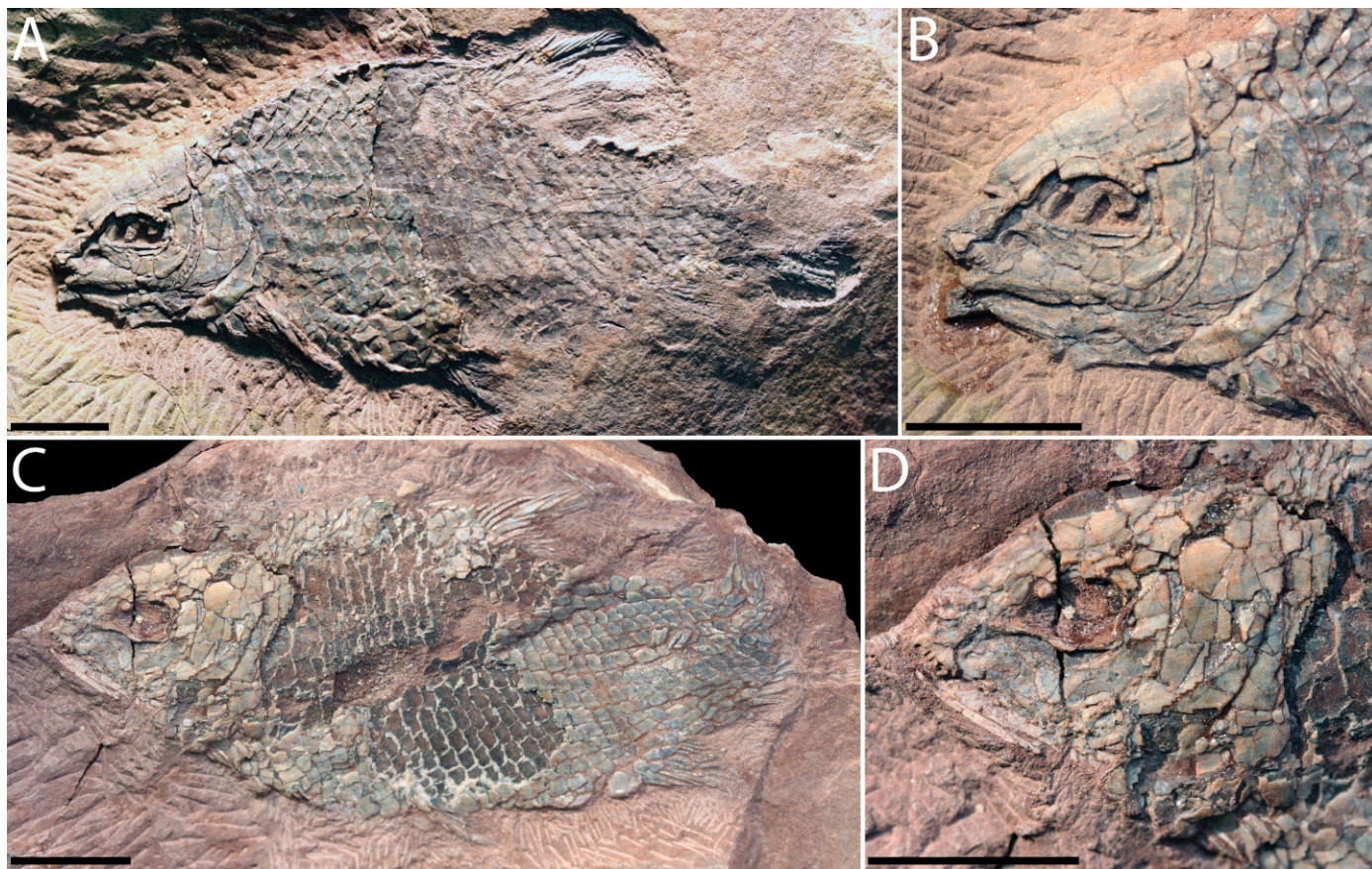


Fig. 2. †*Lophionotus chinleana*, new species, from the Upper Triassic Chinle Formation, UMNH VP 19417 in (A) left lateral view of complete specimen, (B) close-up of skull region; UMNH VP 19418 in (C) left lateral view of complete skeleton, (D) close-up of skull region. All scale bars equal 1 cm.

angle to a thin process that wraps around anterior of snout (Figs. 2BD, 3, 4).

†*Lophionotus chinleana* has a closed circumorbital ring, which is well preserved in UMNH VP 19417 (Figs. 2AB, 3, 4),

UMNH VP 19418 (Fig. 2CD), and AMNH 5682 (Fig. 5). At least two anameric supraorbitals are dorsal to orbit and adjacent to lateral edge of parietal (Fig. 4). Supraorbital bones are narrow and smooth. They articulate posteriorly

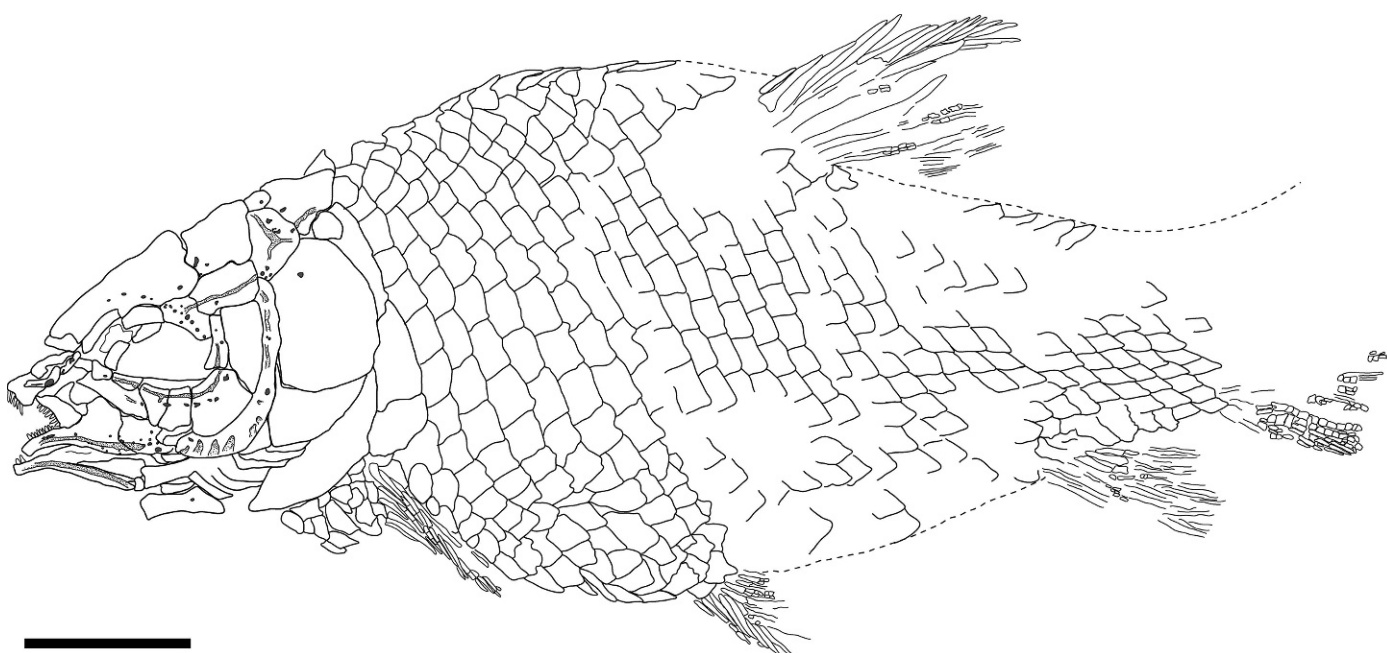


Fig. 3. †*Lophionotus chinleana*, new species, from the Upper Triassic Chinle Formation, UMNH VP 19417 drawing, outline of general body form shown with dashed line, stippled areas on skull indicate preserved sensory canals. Scale bar equals 1 cm.

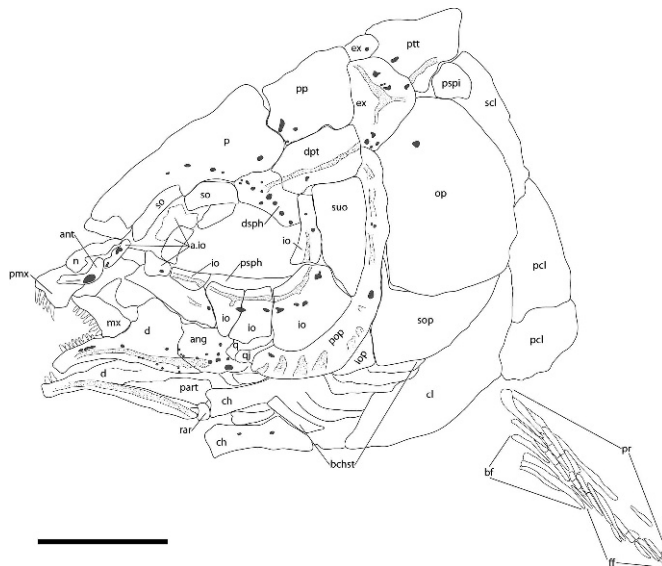


Fig. 4. †*Lophionotus chinleana*, new species, from the Upper Triassic Chinle Formation, UMNH VP 19417 skull in left lateral view. Stippled areas indicate sensory canals preserved on the specimen. Scale bar equals 1 cm.

with dermosphenotic and anteriorly with anterior infraorbitals (Fig. 4).

Dermosphenotic forms posterodorsal corner of the orbital ring and bears juncture of infraorbital canal and temporal canal (Figs. 2–5). Dermosphenotic articulates dorsally with lateral edge of parietal, posteriorly with dermopterotic, and its smaller ventral process articulates with infraorbital posterior to orbit (disarticulated in UMNH VP 19417, Fig. 4).

Five infraorbitals comprise posterior and ventral portions of circumorbital ring, and best preserved in UMNH VP

19417 (Figs. 2AB, 3, 4). A single, narrow infraorbital lies posterior to orbit and articulates with dermosphenotic dorsally, suborbital posteriorly, and larger posteroventral corner infraorbital (disarticulated in Figs. 4, 5). Infraorbital in posteroventral corner of circumorbital ring has narrow anterodorsal process and expands posteroventrally to fill open area below suborbital and anterior ramus of preoperculum (Figs. 2–5). Infraorbitals below orbit are deep; series narrows anteriad. Anteriormost infraorbital is narrow and articulates with anterior infraorbital series (lachrymals or lacrimals of traditional terminology). Exact number of anterior infraorbitals is not known because all elements may not have been preserved. Specimen UMNH VP 19417 has three to four anterior infraorbitals preserved (Fig. 4).

†*Lophionotus chinleana*'s suborbital is wedge-shaped, narrow, and deep; lateral surface is smooth and unornamented (Figs. 2–5). It lies flush with other cheek bones, rather than overlying other dermal bones. Dorsal margin is square-shaped and articulates with anteroventral edge of dermopterotic. Anterior margin is straight and articulates with posterior edges of infraorbital posterior to orbit (Figs. 2–5). Anteroventral margin curves convexly posteroventrad and articulates with concave posterodorsal margin of large infraorbital in posteroventral corner of circumorbital series (Figs. 4, 5), closing "gap" between anterior ramus of the preoperculum and circumorbital series.

Preoperculum is crescent-shaped and best preserved in UMNH VP 19417 (Figs. 2AB, 3, 4) and AMNH 5682 (Fig. 5). Dorsal portion of preoperculum is vertical and rod-like. Ventral and dorsal processes are of about equal length (Figs. 2AB, 3–5). Dorsal process articulates with operculum posteriorly. Anterodorsally, it articulates with wedge-shaped suborbital and infraorbitals. Dorsal margin contacts posteroventral edge of dermopterotic (Figs. 4, 5). As it curves anteroventrad, its posterior margin contacts

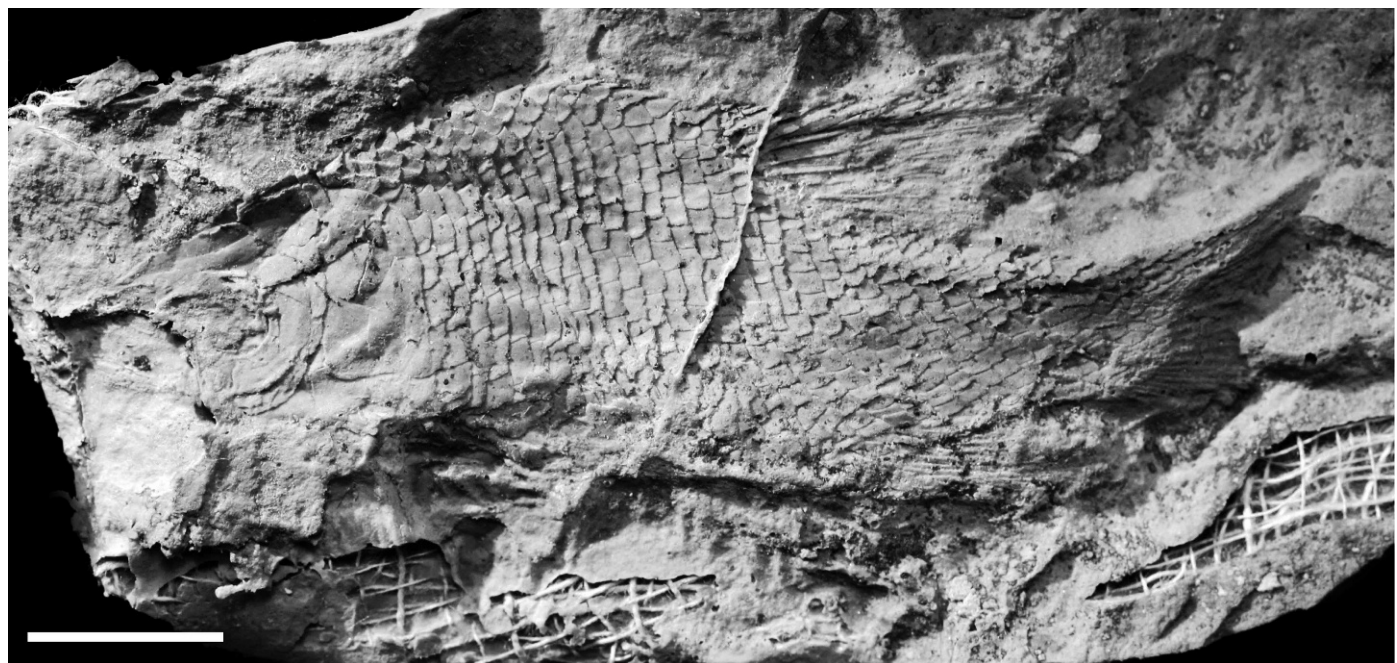


Fig. 5. †*Lophionotus chinleana*, new species, from the Upper Triassic Chinle Formation, AMNH 5682, latex peel of complete specimen in left lateral view. Scale bar equals 1 cm.

ascending process of suboperculum and interoperculum (Figs. 4, 5).

Operculum large and ovoid in shape. Anterior and ventral margins are essentially straight with curving posterior border (Figs. 2–5). Operculum is smooth and lacks ornamentation or ridging. Dorsal border articulates with extrascapular, postspiracular, supracleithrum. Posterior border articulates with supracleithrum and dorsal postcleithrum (Figs. 4, 5).

Suboperculum is overlapped dorsally by ventral margin of operculum. Suboperculum is triangular with curving ventral border that tapers posterodorsad (Figs. 4, 5). Anterior margin contacts interoperculum in a straight suture. A narrow ascending process extends from anterodorsal corner of suboperculum. Exposed depth of suboperculum is about one-third or less than depth of operculum (Fig. 4).

Interoperculum is small and triangular, articulating posteriorly with suboperculum and dorsally overlain by the preoperculum. It has a relatively straight ventral margin (Figs. 2AB, 3–5).

Premaxilla robust with ascending process. Ascending process curves inward from anterior process and is covered by nasal and antorbital bones (Figs. 2–4). Ascending process articulates posterodorsally with anterior margin of parietals (Figs. 2–4). Anterior portion of premaxilla expands horizontally and bears a series of large, conical, blunt teeth (Figs. 2–4).

Maxilla short, narrows anteriad to a small process that articulates with premaxilla beneath antorbitals (Figs. 2AB, 3, 4). Maxilla widens posteriorly and ends with a gently curved margin. Maxilla bears a single row of at least seven teeth along ventral margin. Supramaxilla not preserved in any specimen.

Dentary is narrow and bears at least seven to ten styliform teeth. In labial view, trapezoidal angular articulates anteriorly with posterior margin of dentary with a wavy suture (Fig. 4). In lingual view, dentary has thick ventral "lip" (Figs. 2, 4). Dentary cups mediad and prearticular articulates with dorsal margin of ventral lip of dentary. Prearticular is long and tapers anteriad with shape of labial portion of dentary (Figs. 2BD, 4). Retroarticular is poorly preserved on posterior margin of mandible (Fig. 4).

Quadrato and quadratojugal are preserved in UMNH VP 19417 (Fig. 4). Only ventral portion of quadrato is visible; dorsal portion is overlain by infraorbital series. Posteroventral edge of quadrato forms a strong lip that is strongly appressed to quadratojugal. Quadratojugal is long and splint-like, and rests along the dorsal margin of ventral arm of preoperculum (Fig. 4).

Neurocranial elements are not visible in any specimen of *†L. chinleana*. Ceratohyal is visible on ventral margin, and is robust with expansions at anterior and posterior ends of the bone. Branchiostegals are preserved as a series of long horizontal bones with tapered ends below interoperculum and suboperculum. Five to seven branchiostegals are preserved in UMNH VP 19417 (Figs. 2B, 4).

Supraorbital canal is observed as a row of pores that runs on the lateral edge of the parietals, above articulation with supraorbital bones (Figs. 2B, 3, 4). Canal continues posteriad into postparietals. Supraorbital bones themselves are anameric (Fig. 4).

Preopercular sensory canal is prominent as a deep groove that runs along anterior side of preoperculum (Figs. 2B, 3–5). Ventral arm of preopercular is perforated with a series of ventrally directed grooves, which house exits for branches of preopercular sensory canal (Figs. 3–5). Preopercular sensory

canal exits anteriorly and continues as mandibular sensory canal (Fig. 4).

Mandibular sensory canal runs along ventral ramus of dentary. It is visible in UMNH VP 19417 (Figs. 2AB, 3, 4) and UMNH VP 19418 (Fig. 2CD) as series of elongated pores.

Infraorbital sensory canal begins in dermosphenotic and travels ventrad through infraorbital series, continuing into anterior infraorbitals and antorbitals (Fig. 4). Posterodorsally, infraorbital sensory canal connects to temporal sensory canal in dermosphenotic (Fig. 4). Connection to supraorbital canal in dermosphenotic cannot be directly observed but may be suggested by presence of pores.

Temporal canal begins in dermosphenotic at junction with infraorbital canal. It continues through lateral portion of the dermopterotic and extrascapular. Canal branches into occipital commissure on extrascapular series. Main canal continues on posttemporal and supracleithrum, where it connects with the main lateral line canal on body (Fig. 4).

Cleithrum, postcleithra, and supracleithrum are preserved in lateral aspect. Two postcleithra sit posterior to operculum and cleithrum. Ventral postcleithrum is trapezoidal to triangular in shape (Figs. 2–5). Dorsal edge of ventral postcleithrum articulates in wavy suture with dorsal postcleithrum (Figs. 2–5). Posterior edge of ventral postcleithrum is slightly. Dorsal postcleithrum is deeper than ventral postcleithrum. It tapers dorsad, and it articulates on anterior margin with operculum anterodorsally, cleithrum anteriorly, and supracleithrum dorsally. Supracleithrum lies dorsal to postcleithrum and posterodorsal to operculum. It is elongate, and ventral process articulates with operculum anteriorly and slightly overlies dorsal postcleithrum (Fig. 4). It is also deep and narrow, and tapers ventrad.

Cleithrum is a robust, long, gently curving, anteriorly inclined bone. It lies ventral to suboperculum and interoperculum and extends dorsad between suboperculum anteriorly and postcleithra posteriorly. Dorsal tip of cleithrum may reach below operculum (Fig. 4).

Well-developed basal fulcra precede all fins of *†Lophionotus chinleana*. Fringing fulcra originate on first lepidotrichium. Due to incomplete preservation, exact number of lepidotrichia is not known. Number provided here is an estimate of number of lepidotrichia for each fin.

Pectoral fin is preserved in UMNH VP 19417 (Figs. 2A, 3, 4) and is comprised of at least three basal fulcra and approximately seven fringing fulcra on first lepidotrichium. Number of rays is indeterminable in available specimens but is estimated at five lepidotrichia.

Pelvic fins are preserved in AMNH 5682 (though poorly preserved, Fig. 5), UMNH VP 19417 (Figs. 2A, 3) and UMNH VP 19418 (Fig. 2C). They indicate a ventral origin approximately midway between pectoral fins and anal fin. Pelvic fin has approximately two to three basal fulcra and approximately four to five rays, first ray bearing anywhere from three to six fringing fulcra.

Triangular dorsal fin originates just posterior to origination of pelvic fins. It is comprised of one uniserial fulcral scale and three basal fulcra, each longer than preceding one. Fringing fulcra in dorsal fin of UMNH VP 19417 are well preserved and number approximately ten (Figs. 2A, 3). Dorsal fin has eight to 11 branched, segmented rays.

Anal fin is triangular and is slightly smaller to equal in size to dorsal fin (Figs. 2AC, 3, 5). It originates slightly behind posterior edge of dorsal fin, and has three basal fulcra, five

fringing fulcra, and seven to nine lepidotrichia, becoming segmented distally.

Caudal fin is not completely preserved in any specimen. Specimen AMNH 5682 (Fig. 5) preserves caudal peduncle and dorsal lobe in impression, but distal ends of rays of fin are faintly preserved or not preserved at all. Caudal fin is abbreviated heterocercal (hemiheterocercal). Dorsal lobe of caudal fin has at least four basal fulcra, long and attenuated (Fig. 5). Ventral lobe is poorly preserved but shows at least three to four basal fulcra (Fig. 3). There are approximately seven rays in dorsal lobe, and nine to 11 rays in ventral lobe (Fig. 5).

Endoskeleton is not observed in any specimen. Body is covered with smooth, rhombic scales. Scales on flank are quadrangular and possess typical peg-and-socket articulation, as is observed in occasional disarticulated scales. Scales vary little in size across flank, only becoming smaller and more rhomboidal in area of caudal peduncle (Figs. 2AC, 5). †*Lophionotus chinleana* shows relatively little serration on posterior edge of any flank scales, though this could be due to weathering and preservation of the specimens.

There are approximately 30 scales in lateral line. Lateral line scales are notched on posterior margin; these notches allow for an opening of lateral line canal to surface (Figs. 3, 5).

Dorsal ridge scales are similar to those seen in other semionotiforms, with a prominent, acuminate process that points posteriad. Anterior dorsal ridge scales are shorter with a small process. Scales become more elongated posteriad. Dorsal ridge scales are well preserved in UMNH VP 19417 (Figs. 2A, 3) and AMNH 5682 (Fig. 5). Ventral ridge scales are ovate and large. Dorsal scutes on caudal peduncle between dorsal and caudal fins are ovate and have a small acuminate process on posterior end (Figs. 3, 5).

Type locality.—Walt's Quarry, Lisbon Valley, San Juan County, Utah (Fig. 1).

Age, habitat, and distribution.—†*Lophionotus chinleana*, new species, is found in the Upper Triassic (Norian) Church Rock Member, Chinle Formation. As was discussed previously, the Church Rock Member of the Chinle is interpreted as a freshwater fluvial-lacustrine system. The complete geographic distribution of †*L. chinleana* is unknown.

Etymology.—The specific name *chinleana* refers to the Upper Triassic Chinle Formation, from which specimens of this new species have been recovered.

†*Lophionotus kanabensis* (Schaeffer and Dunkle, 1950)

Kanab Ridgeback
Figures 6, 7; Table 1

†*Semionotus kanabensis* Schaeffer and Dunkle, 1950:3–15

Holotype.—AMNH 8870: complete fish with uncrushed skull (Fig. 6).

Paratypes.—AMNH 8871: dorsoventrally crushed and partly dissociated skull and anterior portion of body (Fig. 7); USNM 18399: laterally compressed skull with well-preserved cheek area and mandible, also section of body including dorsal and anal fins (Schaeffer and Dunkle, 1950:figs. 4, 6); USNM 18400: patches of scales and broken skull elements.

Specific diagnosis.—Revised from Schaeffer and Dunkle (1950) to include only differential diagnostic features. The diagnosis for this species is based upon the unique combination of the following characters: parietals long and narrow (shorter, broad parietals in †*Lophionotus sanjuanensis* and †*L. chinleana*); infraorbitals below the orbit narrower than posteroventral infraorbital (compared to deep infraorbitals of †*L. sanjuanensis*); posteroventral infraorbital articulates directly with dermosphenotic (at least one infraorbital present between dermosphenotic and posteroventral infraorbital in †*L. sanjuanensis* and †*L. chinleana*); no infraorbital posterior to orbit (one infraorbital present in †*L. chinleana*, two infraorbitals present in †*L. sanjuanensis*); preoperculum anteriorly inclined and “boomerang”-shaped (vertically inclined and L-shaped in †*L. sanjuanensis*, vertically inclined and crescent-shaped in †*L. chinleana*); ventral arm of preoperculum wider than dorsal arm (equal width in †*L. chinleana*); suborbital large and rectangular (narrow and wedge-shaped in †*L. chinleana*, narrow in †*L. sanjuanensis*); maxilla edentulous (toothed maxilla in †*L. sanjuanensis* and †*L. chinleana*); single pair extrascapulars, lacking median extrascapular (median extrascapular present in †*L. chinleana*); lacking postspiracular (present in †*L. chinleana*); gently curved dorsal border (lacking postcranial hump seen in †*L. sanjuanensis*); small body size (approximately 50–60 mm in available specimens, compared to average 87.7 mm SL in †*L. sanjuanensis* and average 68 mm SL in †*L. chinleana*); lacking dense tuberculation (tuberculation present in †*L. sanjuanensis*).

Description.—†*Lophionotus kanabensis* is a small fusiform fish with gently curved dorsal border, similar to †*L. chinleana*. Body is either not completely preserved or distorted in available specimens, so estimated SL is between 50–60 mm. Skull is triangular, longer than deep, and HL is 18 mm, about 30% SL.

Skull roof contains a pair of parietals and postparietals. Parietals are long and narrow (approximately two and a half times longer than wide) and comprise majority of skull roof (Figs. 6A–D, 7). Anterior margin is strongly digitate, and articulates with ascending process of premaxilla (Fig. 6A–D). Parietals are widest at posterior margin, constrict over the orbits, and widen anterior to orbital constriction (antorbital process), and taper anterior to antorbital process. Suture between parietals is linear, with some minor sinuous articulation and asymmetry. Parietals articulate with supraorbital and anterior infraorbitals laterally, postparietals posteriorly, and dermopterotic dorsolaterally (Fig. 6).

Postparietals are rectangular and slightly longer than deep. Suture between postparietals is undulous. They articulate with parietals anteriorly, dermopterotic laterally, and extrascapulars posteriorly (Figs. 6A–E, 7).

Dermopterotic is rectangular, longer than deep. Dorsal border articulates with lateral edge of postparietals (Fig. 6D). At anterodorsal corner, dorsal margin curves anteroventrad and articulates with dorsoventral corner of parietal (Fig. 6D).

Extrascapulars are poorly preserved in AMNH 8870 (Fig. 6) and USNM 18399. They are triangular (wider at the lateral margin and tapering medially) and articulate anteriorly with postparietals (Fig. 6C). Posterior to extrascapulars, posttemporals are very poorly preserved or obscured. They may be present in AMNH 8871 (Fig. 7B), but poor preservation makes this difficult to interpret.

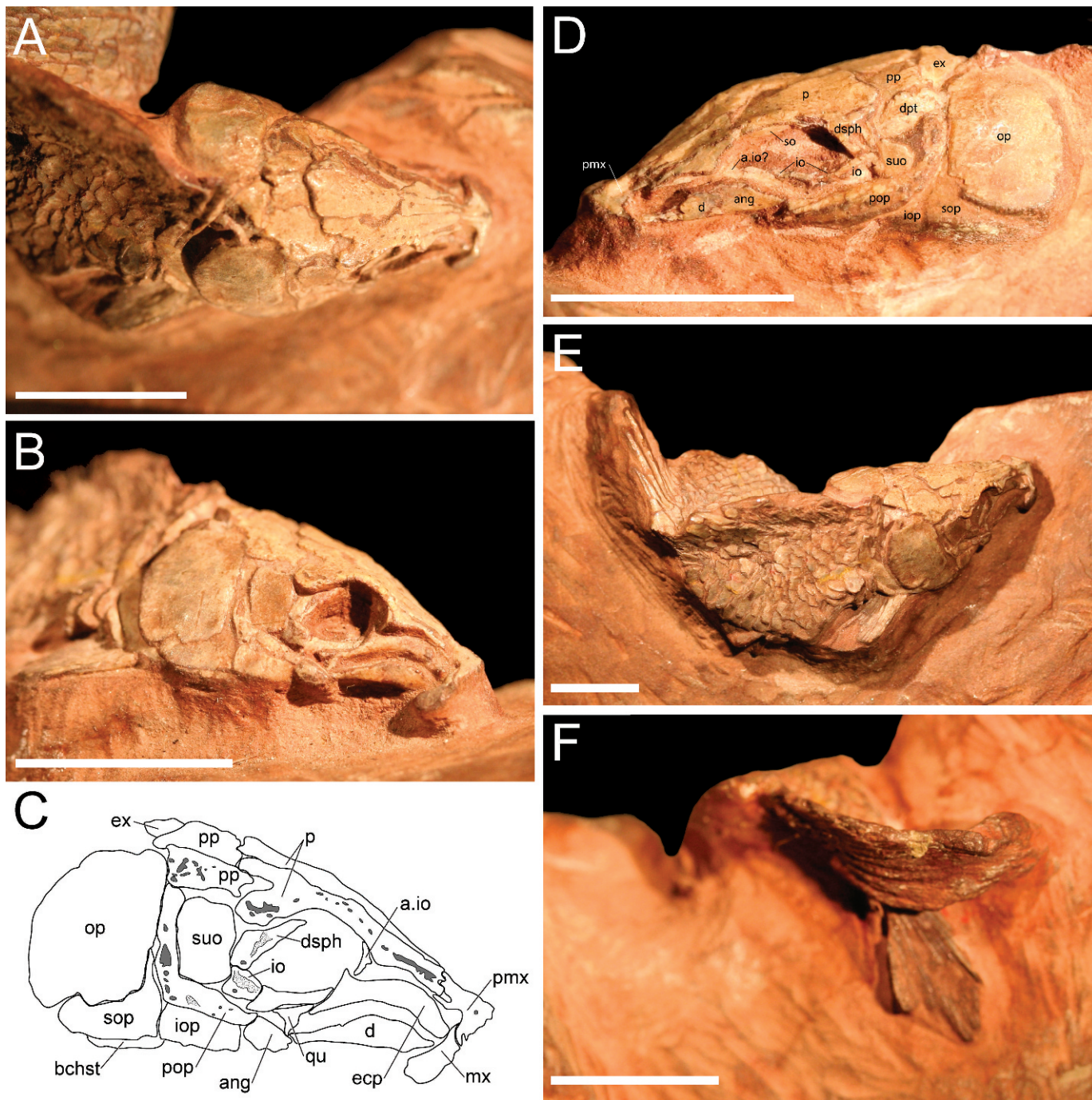


Fig. 6. †*Lophionotus kanabensis* from the Lower Jurassic Moenave Formation. Type specimen AMNH 8870 in (A) dorsal view of skull; (B) right lateral view of skull; (C) drawing of skull right lateral view, stippled areas indicate visible sensory canals, grayed areas indicate sensory pores; (D) left lateral view of skull; (E) right oblique view of complete specimen; (F) ventral view of caudal fin. All scale bars equal approximately 1 cm.

Nasal and rostral bones are not preserved in any specimen of †*Lophionotus kanabensis*. Antorbital bone is preserved as a small fragment in USNM 18399 (Schaeffer and Dunkle, 1950:fig. 6B).

†*Lophionotus kanabensis* has a closed circumorbital ring, but entire series is not preserved in any one specimen. Specimen USNM 18399 retains three poorly preserved elements that are possibly broken elements of a supraorbital (Schaeffer and Dunkle, 1950:figs. 4A, 6B). AMNH 8870 contains one slender supraorbital that articulates with lateral edge of parietal (Fig. 6D).

Dermosphenotic forms posterodorsal corner of orbital ring and bears the junction of the infraorbital and temporal

canals. Dermosphenotic articulates dorsally with lateral edge of the parietal, posteriorly with dermopterotic, and ventrally with expanded infraorbital posteroventral to orbit (Fig. 6CD).

A series of infraorbitals comprise posteroventral and ventral portions of circumorbital ring, best preserved in USNM 18399 (Schaeffer and Dunkle, 1950:fig. 6B) and AMNH 8870 (Fig. 6D). Posteroventral corner infraorbital articulates dorsally with dermosphenotic, is large, and expands ventrally to contact anterior ramus of preoperculum (Fig. 6CD). Infraorbital series continues anterior to posteroventral infraorbital and ventral to orbit (Fig. 6D;

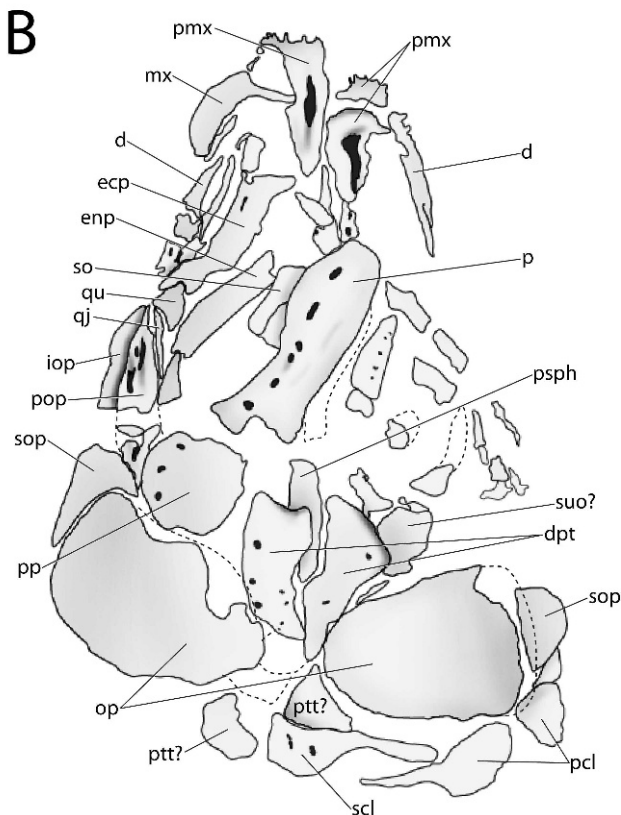


Fig. 7. [†]*Lophionotus kanabensis* from the Lower Jurassic Moenave Formation, AMNH 8871. (A) Skull in dorsal view, (B) drawing of skull in dorsal view. Scale bar equals 1 cm.

Schaeffer and Dunkle, 1950:fig. 6B). These infraorbitals are narrow and articulate with anterior infraorbital series. At least two anterior infraorbitals are present, as seen in USNM 18399 (Schaeffer and Dunkle, 1950:fig. 6B). Schaeffer and Dunkle (1950) interpreted one as a circumorbital, and did not label other anterior infraorbital. An anterior infraorbital is also visible in AMNH 8870 (Fig. 6CD).

[†]*Lophionotus kanabensis* has a single anametic suborbital (Fig. 6). Suborbital is large, rectangular, longer than wide (approximately one and a half to two times longer than wide). Surface of suborbital is smooth and overlies anterior portion of dorsal process of preoperculum. Dorsal edge of suborbital articulates with anteroventral edge of the dermopterotic. Anteriorly, suborbital articulates with dermosphenotic and articulates anteroventrally with posterodorsal corner of expanded infraorbital (Fig. 6BCD). Posteriorly, suborbital articulates with anterior edge of preoperculum.

Preoperculum is anteroventrally inclined and boomerang-shaped. Ventral and dorsal processes are of about equal length (Fig. 6CD). Dorsal process articulates with operculum posteriorly (Fig. 6CD), is overlain by suborbital anteriorly, and contacts posteroventral edge of the dermopterotic on dorsal margin (Fig. 6D). Ventrally, preoperculum contacts ascending process of suboperculum and interoperculum. Anterodorsally, it articulates with suborbital and infraorbital in posteroventral corner of orbit (Fig. 6CD).

Operculum large and oval. Anterior and ventral margins are straight, with curving posterior border (Figs. 6, 7). Dermal surface of operculum is smooth and lacks ornamentation or ridging. Dorsal border articulates with extrascapular; posterior border articulates with supracleithrum and cleithrum (Fig. 6BE); ventral border articulates with suboperculum (Figs. 6BCD, 7).

Suboperculum is overlapped dorsally by ventral margin of operculum (Fig. 7B). Suboperculum is triangular with a curving ventral border that tapers posterodorsad toward posterior of the operculum. Anterior margin articulates with interoperculum. A narrow ascending process extends dorsad from anterodorsal corner of suboperculum. Exposed depth of suboperculum is about one-third or less than depth of operculum (Schaeffer and Dunkle, 1950; Figs. 6BCD, 7).

Interoperculum is a small, rectangular bone, articulating posteriorly with suboperculum and dorsally overlain by preoperculum. It is wider at posterior margin and tapers anteriad. It has a relatively straight ventral margin (Fig. 6BCD).

Premaxilla is well preserved and has a large ascending process that contains a large foramen (Fig. 7). Ascending process curves inward from anterior margin of premaxilla and articulates with strongly digitate anterior margin of parietals (Fig. 6ABCD). Anterior portion of premaxilla expands laterally and bears a series of large, conical, blunt teeth (Figs. 6BCD, 7), numbering around five to seven.

Maxilla is short and edentulous. It narrows anteriad to a small medial process that articulates with premaxilla in a hinge-like manner (Figs. 6, 7). Maxilla widens posteriorly and ends with a gently curved margin (Figs. 6, 7). Supramaxilla is poorly preserved in USNM 18399 and articulates with posterodorsal margin of the maxilla (Schaeffer and Dunkle, 1950:fig. 6B).

Lower jaw is best preserved in USNM 18399 and AMNH 8860 (Fig. 6BCD). Dentary is narrow with a high coronoid process and bears at least seven to ten styliform teeth (Schaeffer and Dunkle, 1950:fig. 6B). Schaeffer and Dunkle

(1950) noted "somewhat procumbent marginal teeth on either side of the symphysis... An inner row of stouter teeth is also present, but their form cannot be determined." In labial view, the trapezoidal angular articulates anteriorly with the posterior margin of the dentary with a strongly digitate suture (Fig. 6D). This suture ends dorsally with the articulation of the surangular, a small triangular bone forming the high coronoid process of the lower jaw (seen in USNM 18399, Schaeffer and Dunkle, 1950:fig. 6B).

Quadrato is seen in AMNH 8870 (Fig. 6C) and AMNH 8871 (Fig. 7B), and is a small, thick triangular element, rounded at mandibular articulation (Fig. 6C). It articulates with a splint-like quadratojugal that rests parallel to anterior edge of preoperculum (Fig. 7B). Schaeffer and Dunkle (1950) identified this quadratojugal as a symplectic (Schaeffer and Dunkle, 1950:fig. 6A). Symplectic is visible in USNM 18399 (Schaeffer and Dunkle, 1950:fig. 6B) beneath infraorbital posteroventral to orbit and anterior to preoperculum.

A few palatal elements are visible in all specimens. Ectopterygoid is narrow and curved convexly (Fig. 6BC). Posterior end is flat with short dorsal process and ventral processes (Fig. 6C). Endopterygoid is seen in AMNH 8871 (Fig. 7B) and USNM 18399 (Schaeffer and Dunkle, 1950:fig. 6B), and is broad and rectangular. Parasphenoid is poorly preserved in USNM 18399 but not labeled in any figure.

Complete hyoid arch is not visible in any specimen. Some elements of hyoid arch are visible in a few of the specimens. Specimen USNM 18399 preserves impression of hyomandibula that was described in Schaeffer and Dunkle (1950) as having an "essentially vertical position and about three times longer than the width at the neurocranial articulation."

Ceratohyal is visible on ventral margin of USNM 18399, and is a robust bone expanded proximally and distally. Schaeffer and Dunkle (1950) identified two poorly preserved ossifications anterior to ceratohyal as hypohyal and "glossohyal," but due to poor preservation they really cannot be identified with such confidence.

Branchiostegals are preserved as a series of long horizontal bones with tapered ends below the interoperculum and suboperculum. Five to seven branchiostegals are preserved in USNM 18399 (Schaeffer and Dunkle, 1950:fig. 6B). A single branchiostegals is preserved in AMNH 8870 (Fig. 6C).

Supraorbital canal is observed as a row of pores that runs on lateral edge of parietals and continues on the lateral edge of the postparietals (Figs. 6ABC, 7).

Preopercular sensory canal is observed as a series of prominent pores (Figs. 6BCD, 7). Ventral arm of preoperculum is perforated with ventrally directed grooves, which house exits for branches of preopercular sensory canal (Figs. 6C, 7B). Preopercular sensory canal exits ventral arm of preoperculum anteriad.

Mandibular canal runs along ventral ramus of mandible. It is visible in USNM 18399 as a series of large, weathered pores (Schaeffer and Dunkle, 1950:fig. 6B).

Infraorbital canal begins in dermosphenotic and travels ventrally through infraorbital series (Fig. 6CD). It is not seen in anterior infraorbitals.

Temporal canal begins in dermosphenotic and continues posteriad through dermopterotic (Figs. 6D, 7B). Remainder of sensory canal not preserved, but continues as main lateral line system of body.

Pectoral girdle is very poorly preserved in all specimens of *†Lophionotus kanabensis*. Supracleithrum is preserved in

AMNH 8870 and AMNH 8871. It lies dorsal to postcleithrum and posterodorsal to operculum. Supracleithrum has a long ventral process that articulates with operculum. It preserves two pores on AMNH 8871 that represent the main lateral canal (Fig. 7B). Cleithrum is long, gently curving, and anteriorly inclined. It lies posterior to suboperculum and operculum (Fig. 6B).

Basal fulcra precede all fins of *†Lophionotus kanabensis*. Fringing fulcra originate on the first lepidotrichium. Due to incomplete preservation and/or missing portions of some specimens, exact number of lepidotrichia is not known. Number provided here is an estimate of number of lepidotrichia for each fin.

The pectoral fin is comprised of at least three basal fulcra and approximately seven to nine rays (Fig. 6E). Pelvic fins are not preserved in any specimen.

Dorsal fin is triangular and originates anterior to origination of anal fin. It is comprised of one uniserial fulcral scale and three basal fulcra, each longer than preceding one, and approximately 11 branched, segmented rays (Fig. 6E; Schaeffer and Dunkle, 1950:fig. 4B).

Anal fin is preserved in USNM 18399, is triangular and slightly smaller than dorsal fin (Schaeffer and Dunkle, 1950:fig. 4B). It has three to four basal fulcra, at least three of which are biserial (Schaeffer and Dunkle, 1950). Anal fin has two to five fringing fulcra, and seven lepidotrichia, becoming segmented distally (Schaeffer and Dunkle, 1950).

Caudal fin is preserved in AMNH 8870, but is twisted as to obscure important details (Fig. 6F). It is reconstructed in Schaeffer and Dunkle (1950:fig. 1). Caudal fin is abbreviated heterocercal (hemiheterocercal).

Endoskeleton is not observed in any specimen. Body is covered with smooth, rhombic scales. Scales on flank are quadrangular and possess peg-and-socket articulation, as is observed in occasional disarticulated scales. Scales vary little in size across the flank (Fig. 6E). Schaeffer and Dunkle (1950) recognized a number of flank scales that show about four fine serrations on posterior edge. Scales along lateral line are not well preserved in any specimen. Dorsal ridge scales are not well preserved in any specimen, but do show a prominent, acuminate process that points posteriad.

Schaeffer and Dunkle (1950) did a histological study of scales of specimens of *†Lophionotus kanabensis*. Scales are composed of a relatively thick, bony layer containing sparse, simple canals (Williamson's Canals) covered by thinner enamel (ganoin). This is a quintessential example of lepidosteoid ganoid scales (Goodrich, 1907).

Type locality.—Near Kanab, Kane County, Utah (approximately Sec.27,T.43S.,R.6W), United States. The original field site was estimated as being one mile east and 400 feet above the old Kanab schoolhouse (Camp, 1930).

Age, habitat, and distribution.—The original specimens of *†Lophionotus kanabensis* (Schaeffer and Dunkle, 1950) were collected in the Lower Jurassic Whitmore Point Member of the Moenave Formation (the Type Horizon). The Whitmore Point is interpreted as a large lacustrine deposit (Wilson, 1967; Milner et al., 2006b). The complete distribution of *†L. kanabensis* is in need of further investigation.

Etymology.—Named for the city of Kanab, Utah, United States, near where the Moenave Formation specimens described by Schaeffer and Dunkle (1950) were found.

Remarks and comparisons.—A distinctive morphology that diagnoses †*Lophionotus* from †*Semionotus* is the ventrally expanded infraorbital series. All other currently described and valid species of †*Semionotus* (e.g., †*Semionotus elegans*, †*Semionotus bergeri*) have a narrow infraorbital series, where the ventral edge does not articulate with any other bones in the skull (Olsen and McCune, 1991:fig. 6). This arrangement leaves an “open” cheek region, exposing the metapterygoid and endopterygoid. †*Lophionotus*, however, differs in that the infraorbitals are enlarged and expanded ventrad and anterior to the suborbital bone. This expansion allows the ventral edge of the infraorbitals to contact the anterior ramus of the preopercular. While this character state is also observed in the Chinese taxa †*Kyphosichthys grandei* (Xu and Wu, 2012) and †*Sangiorgioichthys sui* (López-Arbarello et al., 2011), European taxa †*Lepidotes' microrhysis* (Wenz, 2003), †*Paralepidotus ornatus* (Tintori, 1996), †*Sangiorgioichthys aldae* (Tintori and Lombardo, 2007), †*Semiolepis brembanus* (Lombardo and Tintori, 2008), and the South American taxa †*Araripelepidotes temnurus* (Santos, 1990) and †*Neosemionotus punctatus* (López-Arbarello and Codorniú, 2007), this character, as well as the combination of other shared characters between the taxa (see revised generic diagnosis), confidently defines the species described in this study as belonging to the western United States genus †*Lophionotus*.

Several characters clearly distinguish †*Lophionotus chinleana*, †*Lophionotus kanabensis*, and the previously described species †*Lophionotus sanjuanensis*. †*Lophionotus sanjuanensis* is larger and deeper bodied, with a large, tuberculated, postcranial hump (Gibson, 2013). Both †*L. chinleana* and †*L. kanabensis* are smaller and slender bodied with a gently curving dorsal border and lacking tuberculation. †*L. sanjuanensis* has a distinct preoperculum with a short, broad, paddle-like ventral process (Gibson, 2013), whereas †*L. chinleana* has a vertical crescent-shaped preoperculum and †*L. kanabensis* has a boomerang-shaped, anteriorly inclined preoperculum. †*Lophionotus sanjuanensis* and †*L. chinleana* possess short, broad parietals and more pronounced expanded infraorbitals, whereas in †*L. kanabensis*, the parietals are longer and slender, and only the posteroventral corner infraorbital is expanded, and the infraorbital ventral to the orbit are narrow. There are other differences: †*L. chinleana* has a median extrascapular, whereas only one lateral pair of extrascapulars is preserved in †*L. sanjuanensis* and †*L. kanabensis*.

Adult specimens of †*Lophionotus chinleana* are smaller overall when compared to adult specimens of †*L. sanjuanensis*, in addition to being slender and lacking a postcranial hump and tuberculation. Gibson (2013) identified a juvenile specimen of †*L. sanjuanensis* that, although similar in size to †*L. chinleana*, clearly possess a postcranial hump (though lacking tuberculation), and similar skull morphology as the adult forms of †*L. sanjuanensis* (Gibson, 2013:fig. 7).

Phylogenetic relationships of †Semionotidae.—The parsimony analysis in TNT found the same 16 most parsimonious trees (tree length of 286, consistency index of 0.399, retention index of 0.727) for each of the 20 independent search replicates. The strict consensus and 50-percent majority rule consensus tree from the 16 most parsimonious trees are shown in Figure 8, and are largely consistent with the results of López-Arbarello (2012), indicating a monophyletic Ginglymodi and †Semionotiformes, and with †*Lepidotes* removed from †Semionotiformes and placed within Lepisosteiformes. Unambiguous synapomorphies to all 16 equally

parsimonious trees are plotted on the strict consensus tree (Fig. 8), with symmetric bootstrap group frequencies for each node plotted on the 50-percent majority rule tree (Fig. 8).

Gibson (2013) placed †*Lophionotus* within the order †Semionotiformes, and the results of this study indicate that the genus †*Lophionotus* is monophyletic and sister to the genus †*Semionotus*. The genus †*Lophionotus* is herein recognized as belonging to the family †*Semionotidae* (†*Lophionotus* and †*Semionotus*) based on the following synapomorphic characters: presence of a triangular lateral expansion of antorbital portion of parietal (frontal), presence of large basal fulcra in the dorsal and anal fins, and presence of dorsal ridge scales with a conspicuous high spine (Fig. 8). The genus †*Lophionotus* is supported by the two unambiguous synapomorphies 23 and 36, with a clade comprised of the Late Triassic species †*L. sanjuanensis* and †*L. chinleana* sister to the Early Jurassic species †*L. kanabensis* (Fig. 8). Within the genus †*Semionotus*, the eastern United States species †*S. elegans* is the sister group to a clade that includes the African species †*S. capensis* and the European species †*S. bergeri* (Fig. 8).

The work in this study furthers our knowledge of extinct biodiversity. It also clearly shows the need for continued collecting and taxonomic work, which in turn provide new insights into the evolutionary relationships of extinct and modern fishes.

MATERIAL EXAMINED

†*Araripelepidotes temnurus*: AMNH 19067 CP, 11813; FMNH PF 11835, PF 11849, PF 11852, PF 11853, PF 14043, PF 14349.

†*Callipurbeckia notopterus*: FMNH UF 539.

†*Dapedium pholidotus*: FMNH P 25056, UC 2056.

†*Dapedium punctatus*: FMNH PF 25433.

†*Hemicalypterus weiri*: AMNH 5709–5718.

†*Lepidotes elvensis*: FMNH P 25095.

†*Lepidotes gigas*: FMNH PF 5367.

†*Lepidotes* sp.: FMNH PF 12564, PF 15470.

†*Lophionotus chinleana*: AMNH 5682, 5683; UMNH VP 19417, 19418, 19428.

†*Lophionotus kanabensis*: AMNH 8870 (holotype), 8871; USNM 18399.

†*Lophionotus sanjuanensis*: AMNH 5679, 5680, 5684, 5690; UMNH VP 19419–19421.

†*Semionotus capensis*: AMNH 8828, 8829, 19702; FMNH P 25053–25056.

†*Semionotus elegans*: FMNH P 12751, UC 2060, UF 551; NMMNHS P-15501, P-15503, P-15504, P-15506, P-15536, P-15539, P-15546, P-15548, P-15554, P-15560, P-15563, P-15593, P-15595, P-15598, P-15600.

†*Semionotus fultus*: FMNH UF 958.

†*Semionotus micropterus*: FMNH PF 13104, UC 2059, UF 37.

†*Semionotus tenuiceps*: FMNH P 12548, P 25049, PF 13105, PF 25050–25052, UF 431.

†*Semionotus* sp.: AMNH 5681–5683, 5686–5689, 5691–5696, 5698, 5699, 5702, 5703, 5705–5707, 18970–18972; FMNH

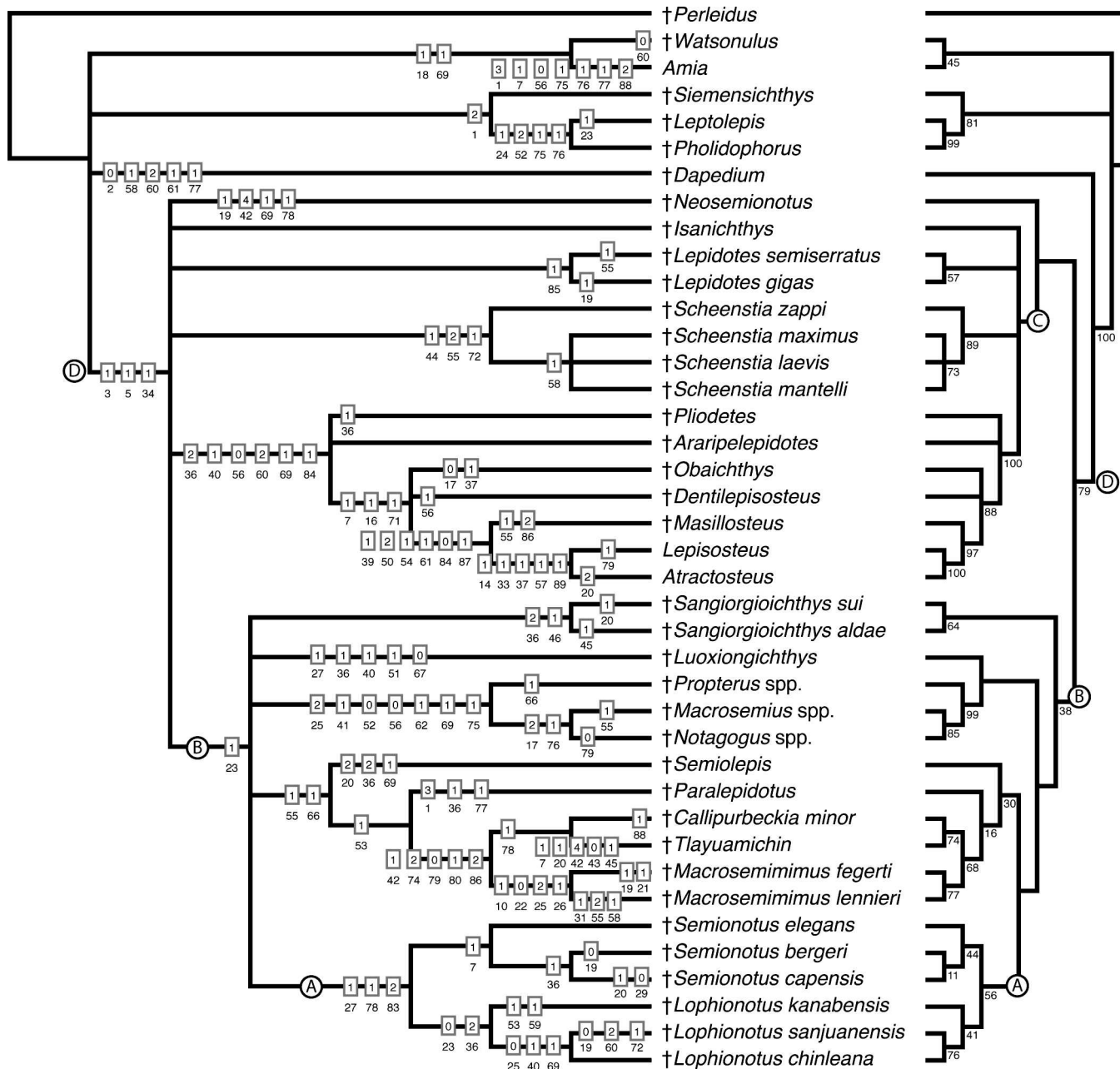


Fig. 8. Phylogenetic relationships of ginglymodian fishes based on a strict (left) and 50-percent majority rule (right) consensus tree from 16 equally parsimonious trees. Unambiguous synapomorphies occurring in each of the 16 trees are indicated on the strict consensus, with symmetric bootstrap frequencies for clades indicated on the 50-percent majority rule consensus tree. (A) †Semionotidae; (B) †Semionotiformes; (C) Lepisosteiformes; (D) Ginglymodi.

PF 5732, PF 13106, PF 151567, UC 2006, UF 452–458, UF 957; NMMNHS P-4184, P-4185, P-17199, P-17254, P-17312, P-22055, P-22065, P-22066, P-22068, P-22069, P-22077, P-22087, P-22088, P-29043, P-32672, P-32673, P-32682, P-32683, P-32684, P-32687, P-32689, P-35423, P-35424, P-35429, P-35430, P-35431, P-44698; SGDS 886, 894, 1059, 1237, 1241, 1314; UMNH VP 19413–19418, VP 19422–19427, VP 19429–19443.

†*Tetragonolepis semicinctus*: FMNH UF 36.

ACKNOWLEDGMENTS

I thank A. Milner (SGDS), J. Kirkland (Utah Geological Survey), J. Maisey (AMNH), and R. Irmis and M. Getty

(UMNH) for use of specimens in this study. Thanks to H.-P. Schultze and G. Arratia for their aid in identification of characters. Thanks to H.-P. Schultze and M. Davis for constructive suggestions for improvement of this manuscript, and M. Davis was also very helpful in performing the phylogenetic analyses in this study. I also thank M. Newbrey for providing insightful comments and suggestions. Thanks to the following institutions: AMNH; Bureau of Land Management, Salt Lake City, Utah; Utah Department of Natural Resources, Salt Lake City, Utah; UMNH; NMMNHS; SGDS; University of Kansas Biodiversity Institute, Lawrence, Kansas; and the Utah Geological Survey, Salt Lake City, Utah. Special thanks to the volunteers from the Utah Friends of Paleontology for their dedicated help in collecting and preparing specimens from Lisbon Valley. This research

was funded in part by the University of Kansas Biodiversity Institute Panorama Grant and National Geographic grant #9071-12. Specimens collected for this study were collected under Utah State Institutional Trust Lands Administration permits 02-334 and 05-347.

LITERATURE CITED

Agassiz, L. 1833–1843. *Recherches sur les Poissons Fossiles*. Volume 2, Part 1. Published by the author, printed by Petitpierre: Neuchâtel et Soleure: VIII, 306.

Arambourg, C., and L. Bertin. 1958. Super-Ordres des Holostéens et des Halécostomes (Holostei et Halecostomi), p. 2173–2203. *In: Traité de Zoologie* 13(3). P. Grassé (ed.). Masson et Cie, Paris.

Arratia, G. 1999. The monophyly of Teleostei and stem-group teleosts. Consensus and disagreements, p. 265–334. *In: Mesozoic Fishes 2—Systematics and the Fossil Record*. G. Arratia and H.-P. Schultze (eds.). Verlag Dr. Friedrich Pfeil, München, Germany.

Arratia, G. 2008. Actinopterygian postcranial skeleton with special reference to the diversity of fin ray elements, and the problem of identifying homologies, p. 49–101. *In: Mesozoic Fishes 4—Homology and Phylogeny*. G. Arratia, H.-P. Schultze, and M. V. H. Wilson (eds.). Verlag Dr. Friedrich Pfeil, München, Germany.

Bartram, A. W. H. 1977. The Macrosemiidae, a Mesozoic family of holostean fishes. *Bulletin of the British Museum of Natural History, Geology* 29:137–234.

Blakey, R. 1989. Triassic and Jurassic geology of southern Colorado Plateau. *In: Geologic Evolution of Arizona*. J. P. Jenney and S. J. Reynolds (eds.). Arizona Geological Society Digest 17:369–396.

Blakey, R., and R. Gubitosa. 1983. Late Triassic paleogeography and depositional history of the Chinle Formation, southern Utah and northern Arizona, p. 57–76. *In: Mesozoic Paleogeography of West-Central United States*. M. W. Reynolds and E. D. Dolly (eds.). Society of Economic Paleontologists and Mineralogists, Rocky Mountain Section, Denver.

Brito, P. M. 1997. Révision des Aspidorhynchidae (Pisces, Actinopterygii) du Mésozoïque: ostéologie, relations phylogénétiques, données environnementales et biogéographiques. *Geodiversitas* 19:681–772.

Camp, C. L. 1930. A study of the phytosaurs. *Memoirs of the University of California* 10:1–174.

Cavin, L. 2010. Diversity of Mesozoic semionotiform fishes and the origin of gars (Lepisosteidae). *Naturwissenschaften* 97:1035–1040.

Cavin, L., and V. Suteethorn. 2006. A new semionotiform (Actinopterygii, Neopterygii) from Upper Jurassic-Lower Cretaceous deposits of north-east Thailand, with comments on the relationships of semionotiforms. *Palaeontology* 49:339–353.

Coates, M. I. 1999. Endocranial preservation of a Carboniferous actinopterygian from Lancashire, UK, and the interrelationships of primitive actinopterygians. *Philosophical Transactions of the Royal Society of London B* 345:435–462.

Cope, E. D. 1872. Observations on the systematic relations of the fishes. *Proceedings of the American Society for the Advancement of Science* 20:317–343.

Deecke, W. 1889. Ueber Fische aus verschiedenen Horizonten der Trias. *Palaeontographica* 35:13–138.

Dubiel, R. F. 1987. Sedimentology of the Upper Triassic Chinle Formation, southeastern Utah: paleoclimatic implications. *Journal of the Arizona–Nevada Academy of Science* 22:35–45.

Eastman, C. R. 1917. Fossil fishes in the collection of the United States National Museum. *Proceedings of the United States National Museum* 52:235–304.

Forey, P. L., A. López-Arbarello, and N. Macleod. 2011. A new species of *Lepidotes* (Actinopterygii: Semionotiformes) from the Cenomanian (Upper Cretaceous) of Morocco. *Palaeontologia Electronica* 14:1–12.

Fraas, O. 1861. Über *Semionotus* und einige Keuper-Conchylien. *Jahreshefte des Vereins für Vaterländische Naturkunde von Württemberg* 17:81–101.

Gallo, V., and P. M. Brito. 2005. An overview of Brazilian semionotids, p. 253–264. *In: Mesozoic Fishes 3—Systematics, Paleoenvironments and Biodiversity*. G. Arratia and A. Tintori (eds.). Verlag Dr. Friedrich Pfeil, München, Germany.

Gardiner, B. G. 1993. Osteichthyes: basal actinopterygians, p. xvii, 611–619. *In: The Fossil Record 2*. M. J. Benton (ed.). Chapman & Hall, London.

Gardiner, B. G., J. G. Maisey, and T. J. Littlewood. 1996. Interrelationships of basal neopterygians, p. 117–146. *In: Interrelationships of Fishes*. M. L. Stiassny, L. R. Parenti, and G. D. Johnson (eds.). Academic Press, San Diego.

Gibson, S. Z. 2013. A new hump-backed ginglymodian fish (Neopterygii: Semionotiformes) from the Upper Triassic Chinle Formation of southeastern Utah. *Journal of Vertebrate Paleontology* 33:1037–1050.

Goloboff, P. A., J. S. Farris, M. Källersjö, B. Oxelmann, M. Ramírez, and C. Szumik. 2003. Improvements to resampling measures of group support. *Cladistics* 19:324–332.

Goloboff, P. A., J. S. Farris, and K. C. Nixon. 2008. TNT, a free program for phylogenetic analysis. *Cladistics* 24: 774–786.

Goodrich, E. S. 1907. On the scales of fish, living and extinct, and their importance in classification. *Proceedings of the Zoological Society of London* 77:751–774.

Grande, L. 2010. An empirical synthetic pattern study of gars (Lepisosteiformes) and closely related species, based mostly on skeletal anatomy. The resurrection of Holostei. *American Society of Ichthyologists and Herpetologists Special Publication 6*.

Grande, L., and W. E. Bemis. 1998. A comprehensive phylogenetic study of amiiid fishes (Amiidae) based on comparative skeletal anatomy. An empirical search for interconnected patterns of natural history. *Society of Vertebrate Paleontology Memoir 4*.

Jain, S. L. 1983. A review of the genus *Lepidotes* (Actinopterygii: Semionotiformes) with special reference to the species from the Kota Formation (Lower Jurassic), India. *Journal of the Palaeontological Society of India* 28:7–42.

Jollie, M. 1986. A primer of bone names for the understanding of the actinopterygian head and pectoral girdle skeletons. *Canadian Journal of Zoology* 64:365–379.

Lambers, P. H. 1999. The actinopterygian fish fauna of the Late Kimmeridgian and Early Tithonian ‘Plattenkalke’ near Solnhofen (Bavaria, Germany: state of the art.). *Geologie en Mijnbouw* 78:215–229.

Larsonneur, C. 1964. *Semionotus normanniae* du Trias supérieur de Basse-Normandie (France). *Annales de Paléontologie* 50:101–117.

Lombardo, C., and A. Tintori. 2008. A new semionotid fish (Actinopterygii: Osteichthyes from the Late Triassic of northern Italy, p. 129–142. *In: Mesozoic Fishes 4—Homology and Phylogeny*. G. Arratia, H.-P. Schultze, and M. V. H. Wilson (eds.). Verlag Dr. Friedrich Pfeil, München, Germany.

López-Arbarello, A. 2004. The record of Mesozoic fishes from Gondwana (excluding India and Madagascar), p. 597–624. *In: Mesozoic Fishes 3—Systematics, Paleoenvironments and Biodiversity*. G. Arratia and A. Tintori (eds.). Verlag Dr. Friedrich Pfeil, München, Germany.

López-Arbarello, A. 2008. Revision of *Semionotus bergeri* Agassiz, 1833 (Upper Triassic, Germany) with comments on the taxonomic status of *Semionotus* (Actinopterygii, Semionotiformes). *Paläontologische Zeitschrift* 82:40–54.

López-Arbarello, A. 2012. Phylogenetic interrelationships of ginglymodian fishes (Actinopterygii: Neopterygii). *PLoS ONE* 7(7):e39370. doi: 10.1371/journal.pone.0039370.

López-Arbarello, A., and J. Alvarado-Ortega. 2011. New semionotiform (Neopterygii) from the Tlayúa Quarry (Early Cretaceous, Albian), Mexico. *Zootaxa* 2749:1–24.

López-Arbarello, A., and L. Codorniú. 2007. Semionotids (Neopterygii, Semionotiformes) from the Lower Cretaceous Lagarcito Formation, San Luis Province, Argentina. *Journal of Vertebrate Paleontology* 27:811–826.

López-Arbarello, A., O. W. M. Rauhut, and K. Moser. 2008. Jurassic fishes of Gondwana. *Revista de la Asociación Geológica Argentina* 63:586–612.

López-Arbarello, A., Z.-Y. Sun, E. Sferco, A. Tintori, G.-H. Xu, Y.-L. Sun, F.-X. Wu, and D.-Y. Jiang. 2011. New species of *Sangiorgioichthys* Tintori and Lombardo, 2007 (Neopterygii, Semionotiformes) from the Anisian of Luoping (Yunnan Province, South China). *Zootaxa* 2749:25–39.

Maddison, W. P., and D. R. Maddison. 2010. Mesquite: a modular system for evolutionary analysis. Version 2.73. <http://www.mesquiteproject.org>

McCune, A. R. 1986. A revision of *Semionotus* (Pisces: Semionotidae) from the Triassic and Jurassic of Europe. *Paleontology* 29:212–213.

McCune, A. R. 1987. Toward the phylogeny of a fossil species flock: semionotid fishes from a lake deposit in the Early Jurassic Towaco Formation, Newark Basin. *Bulletin of the Peabody Museum of Natural History, Yale University* 43:1–108.

McCune, A. R. 2004. Diversity and speciation of semiontid fishes in Mesozoic Rift Lakes, p. 362–379. *In: Adaptive Speciation*. U. Dieckmann, M. Doebeli, J. A. J. Metz, and D. Tautz (eds.). Cambridge University Press, Cambridge, U.K.

Milner, A. R. C., and J. I. Kirkland. 2006. Preliminary review of the Early Jurassic (Hettangian) freshwater Lake Dixie fish fauna in the Whitmore Point Member, Moenave Formation in Southwest Utah. *In: The Triassic-Jurassic Terrestrial Transition*. J. D. Harris, S. G. Lucas, J. A. Spielmann, M. G. Lockley, A. R. C. Milner, and J. I. Kirkland (eds.). New Mexico Museum of Natural History and Science Bulletin 37: 510–521.

Milner, A. R. C., J. I. Kirkland, and T. A. Birthisell. 2006b. The geographic distribution and biostratigraphy of Late Triassic-Early Jurassic freshwater fish faunas of the southwestern United States. *In: The Triassic-Jurassic Terrestrial Transition*. J. D. Harris, S. G. Lucas, J. A. Spielmann, M. G. Lockley, A. R. C. Milner, and J. I. Kirkland (eds.). New Mexico Museum of Natural History and Science Bulletin 37:522–529.

Milner, A. R. C., D. L. Mickelson, J. I. Kirkland, and J. D. Harris. 2006a. A reinvestigation of Late Triassic fish sites in the Chinle Group, San Juan County, Utah: new discoveries. *In: A Century of Research at Petrified Forest National Park: Geology and Paleontology*. W. G. Parker, S. R. Ash, and R. B. Irmis (eds.). Museum of Northern Arizona Bulletin 62:163–165.

Newberry, J. S. 1888. Fossil fishes and fossil plants of the Triassic rocks of New Jersey and the Connecticut Valley. *Monograph of the United States Geological Survey* 14:1–152.

Olsen, P. E. 1984. The skull and pectoral girdle of the parsemionotid fish *Watsonulus eugnathoides* from the Early Triassic Sakamena Group of Madagascar, with comments on the relationships of holostean fishes. *Journal of Vertebrate Paleontology* 4:481–499.

Olsen, P. E., and A. R. McCune. 1991. Morphology of the *Semionotus elegans* species group from the Early Jurassic part of the Newark Supergroup of eastern North America, with comments on the family Semionotidae (Neopterygii). *Journal of Vertebrate Paleontology* 11:269–292.

Patterson, C. 1975. The braincase of pholidophorid and leptolepid fishes, with a review of the actinopterygian braincase. *Philosophical Transactions of the Royal Society of London, Series B* 269:275–579.

Regan, C. T. 1923. The skeleton of *Lepidosteus*, with remarks on the origin and evolution of the lower neopterygian fishes. *Proceedings of the Zoological Society of London* 93:445–461.

Santos, R. S. 1990. Nova conceituação genérica de *Lepidotes temnurus* Agassiz, 1841 (Pisces Semionotiformes). *Anais da Academia Brasileira de Ciências* 62:239–249.

Schaeffer, B. 1967. Late Triassic fishes from the western United States. *Bulletin of the American Museum of Natural History* 135:289–342.

Schaeffer, B., and D. H. Dunkle. 1950. A semionotid fish from the Chinle Formation, with consideration of its relationships. *American Museum Novitates* 1457:1–30.

Schultze, H.-P. 2008. Nomenclature and homologization of cranial bones in actinopterygians, p. 23–48. *In: Mesozoic Fishes 4—Homology and Phylogeny*. G. Arratia, H.-P. Schultze, and M. V. H. Wilson (eds.). Verlag Dr. Friedrich Pfeil, München, Germany.

Stewart, J. H., F. G. Poole, and R. F. Wilson. 1972. Stratigraphy and origin of the Upper Triassic Chinle Formation and related Upper Triassic strata in the Colorado Plateau region. *U.S. Geological Survey Professional Paper* 690.

Su, D. Z. 1996. A new semionotid fish from the Jurassic of Sihuan Basin and its biostratigraphic significance. *Vertebrata Palasitica* 34:91–101.

Thies, D. 1989. *Lepidotes gloriae*, sp. nov. (Actinopterygii: Semionotiformes) from the Late Jurassic of Cuba. *Journal of Vertebrate Paleontology* 9:18–40.

Tintori, A. 1996. *Paralepidotus ornatus* (Agassiz 1833–43): a semionotid from the Norian (Late Triassic) of Europe, p. 167–179. *In: Mesozoic Fishes—Systematics and Paleobiology*. G. Arratia and G. Viohl (eds.). Verlag Dr. Friedrich Pfeil, München, Germany.

Tintori, A., and C. Lombardo. 2007. A new early Semionotidae (Semionotiformes, Actinopterygii) from the upper Ladinian of Monte San Giorgio area (southern Switzerland and northern Italy). *Rivista Italiana di Paleontologia e Stratigrafia* 113:369–381.

Wenz, S. 1968. Compléments à l'étude des poissons actinopterygiens du Jurassique français. *Cahiers Paléontologie*. Centre National de la Recherche Scientifique, Paris.

Wenz, S. 1999. *Pliodetes nigeriensis*, gen. nov. et sp. nov., a new semionotid fish from the Lower Cretaceous of Gadoufaoua (Niger Republic): phylogenetic comments, p. 107–120. In: Mesozoic Fishes 2—Systematics and the Fossil Record. G. Arratia and H.-P. Schultze (eds.). Verlag Dr. Friedrich Pfeil, München, Germany.

Wenz, S. 2003. Les *Lepidotes* (Actinopterygii, Semionotiformes) du Crétacé inférieur (Barrémien) de Las Hoyas (Province de Cuenca, Espagne). *Geodiversitas* 25:481–499.

Wenz, S., P. Bernier, G. Barale, J. P. Bourseau, E. Buffetaut, C. Galliard, and J. C. Gall. 1994. L'ichthyo-faune des calcaires lithographiques du Kimméridgien supérieur de Cerin (Ain, Frans). *Geobios* 16:61–70.

Wiley, E. O. 1976. The phylogeny and biogeography of fossil and recent gars (Actinopterygii: Lepisosteidae). University of Kansas Miscellaneous Publications 64:1–111.

Wiley, E. O. 2008. Homology, identity, and transformation, p. 9–21. In: Mesozoic Fishes 4—Homology and Phylogeny. G. Arratia, H.-P. Schultze, and M. V. H. Wilson (eds.). Verlag Dr. Friedrich Pfeil, München, Germany.

Wilson, R. F. 1967. Whitmore Point, a new member of the Moenave Formation in Utah and Arizona. *Plateau* 40:29–40.

Woodward, A. S. 1890. The fossil fishes of the Hawkesbury Series at Gosford. *Memoirs of the Geological Survey of New South Wales (Palaeontological Series)* 4:i–xiii, 1–56.

Xu, G.-H., and F. Wu. 2012. A deep-bodied ginglymodian fish from the Middle Triassic of eastern Yunnan Province, China, and the phylogeny of lower neopterygians. *Chinese Science Bulletin* 57:111–118.